The Canadian Mineralogist
Vol. 34, pp. 779-801 (1996)

OCCURRENCE AND COMPOSITIONS OF SOME Ti-BEARING MINERALS IN THE STRANGE LAKE INTRUSIVE COMPLEX, QUEBEC–LABRADOR BOUNDARY[1]

TYSON C. BIRKETT[2]

Geological Survey of Canada, Quebec Geoscience Centre, P.O. Box 7500, Sainte-Foy, Quebec G1V 4C7

WALTER E. TRZCIENSKI, JR.

Département de Géologie, Université de Montréal, Case postale 6128, Succursale Centre-Ville, Montreal, Quebec H3C 3J7

JOHN A.R. STIRLING

Geological Survey of Canada, 601 Booth Street, Ottawa, Ontario K1A 0E8

ABSTRACT

Ilmenite, bafertisite and Ti-bearing silicates of the Strange Lake peralkaline granite complex, Quebec–Labrador boundary, preserve a history of crystallization and reaction with the residual magma. Early-formed ilmenite and aenigmatite progressively gave way to astrophyllite, neptunite, and narsarsukite. Sodic amphibole and pyroxene were also involved in the reactions. The entry of Nb into the Na–Ti-silicates can be modeled by $\mathrm{Nb}R^{3+}(R^{4+})_{-2}$. Fe^{3+} also entered the minerals through the model substitution $R_2^{3+}(R^{4+}R^{2+})_{-1}$, and, with fluorine, through $R^{3+}\mathrm{F}(R^{4+}\mathrm{O})_{-1}$. Neptunite was found to accept Nb, F and Fe^{3+} in its structure. Crystal sorting of Ti-silicates, including an unidentified silicocarbonate, may have influenced the evolution of the magma.

Keywords: aenigmatite, astrophyllite, bafertisite, ilmenite, narsarsukite, neptunite, peralkaline granite complex, Strange Lake, Quebec, Labrador.

SOMMAIRE

Dans le granite hyperalcalin de Strange Lake, sur la frontière entre le Québec et le Labrador, l'ilménite, la bafertisite et les minéraux silicatés de Ti temoignent de la cristallisation progressive du magma et de réactions avec le magma résiduel. L'ilménite et l'aenigmatite sont des phases précoces qui ont progressivement cédé leur place à l'astrophyllite, la neptunite et la narsarsukite. L'amphibole et le pyroxène sodiques étaient également impliqués dans ces réactions. L'incorporation du Nb dans les silicates de Na et Ti peut être expliquée par le couple $\mathrm{Nb}R^{3+}(R^{4+})_{-2}$. De même, l'incorporation du Fe^{3+} se fait par une substitution de type $R_2^{3+}(R^{4+}R^{2+})_{-1}$ et, avec le F, par une substitution de type $R^{3+}\mathrm{F}(R^{4+}\mathrm{O})_{-1}$. La neptunite incorpore Nb, F, et Fe^{3+} dans sa structure cristalline. Le triage des silicates de Ti a pu influencer l'evolution magmatique.

Mots-clés: aenigmatite, astrophyllite, bafertisite, ilmenite, narsarsukite, neptunite, granite hyperalcalin, Strange Lake, Québec, Labrador.

INTRODUCTION

Titanium-bearing minerals are commonly among the early-crystallizing phases in peralkaline rocks. Mineral assemblages with aenigmatite or astrophyllite have been used to constraint oxygen fugacity (Nicholls & Carmichael 1969, Marsh 1975). The Ti-bearing minerals in general concentrate the high-field-strength elements in magmas (*e.g.*, Green & Pearson 1987), and thus their fractionation by crystal sorting may strongly influence the trace-element profiles of derivative magmatic liquids. Before Ti-minerals can be included in models of petrogenesis, systematic studies of their occurrence, petrography and chemistry are required. Here, we report on the Ti-bearing minerals in the least-evolved portion of the Strange Lake plutonic complex, Quebec–Labrador. In common with many other peralkaline rocks, a wide variety of Ti-bearing

---

[1] Geological Survey of Canada contribution number 67794.

[2] Present address: SOQUEM, 2600, boulevard Laurier, Sainte-Foy, Quebec G1V 4M6.

minerals are found: aenigmatite (Ang), astrophyllite (Ast), bafertisite (Bft), ilmenite (Ilm), neptunite (Npt), and narsarsukite (Nrs). Other Ti-bearing minerals that have been identified at Strange Lake include arfvedsonite (Arf), aegirine (Ae), titanite and pyrochlore, but these minerals will not be considered in detail here. Three previously unknown phases encountered also have been analyzed by electron microprobe. Mineral symbols follow Kretz (1983). Mineral compositions are derived from basic formulae by the use of the vector method of Burt (1988) and are condensed, where possible, down vectors of isovalent substitution (*e.g.*, combining Fe^{3+}, Al, Cr, Ce, *etc.*, as a single component).

GEOLOGICAL SETTING

The Strange Lake intrusive complex, located some 250 km from Schefferville (Fig. 1), was first recognized in 1979 by geologists of the Iron Ore Company of Canada. The post-tectonic nature of the peralkaline granite complex and its enclosed

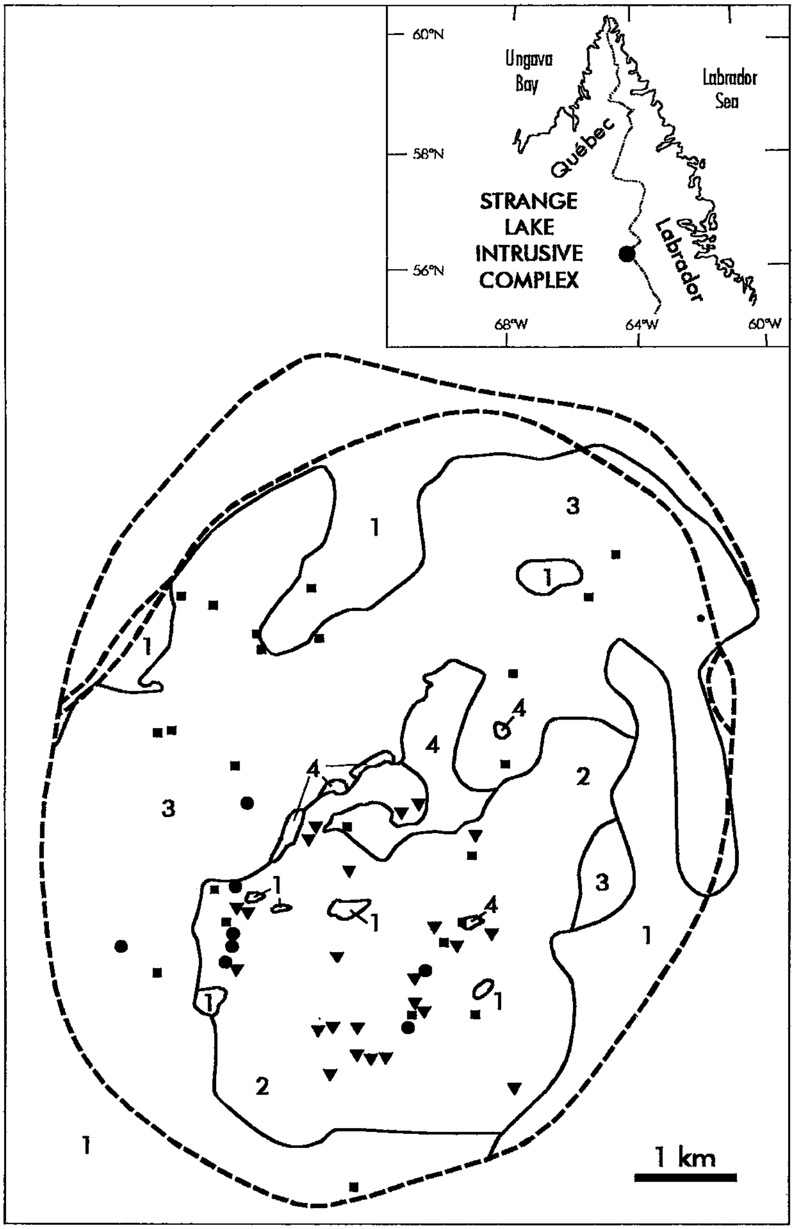

FIG. 1. Simplified geological map of the Strange Lake intrusive body showing the distribution of the various Ti-bearing minerals. The heavy dashed lines represent faults, and the light solid lines, intrusive contacts. The rock units are indicated by numbers: 1 country rock, 2 early hypersolvus granites, 3 middle transsolvus granite, 4 late subsolvus granite and pegmatite–aplite dykes. The distribution of the Ti-bearing minerals is indicated by symbols. Closed circles indicate no Ti-bearing minerals observed; triangles represent assemblages of astrophyllite, aenigmatite, neptunite ± ilmenite; squares represent narsarsukite or titanite.

rare-metals deposit were quickly recognized (Miller 1986). The magmatic evolution preserved in the rocks is from relatively high-temperature hypersolvus units, through subsolvus, rare-metal enriched phases, to low-temperature, extremely enriched pegmatite–aplite dykes. The Strange Lake pluton was described geologically by Zajac *et al.* (1984a, b), Currie (1985), Miller (1985, 1986, 1988, 1990), Birkett & Miller (1991), Pillet (1989) and Pillet *et al.* (1992, 1993). Detailed studies include those of Jambor *et al.* (1987) on armstrongite, Roelofsen-Ahl & Peterson (1989) on the crystal structure of gittinsite, Birkett *et al.* (1992) on the Zr-bearing minerals, Nassif & Martin (1991, 1992) and Nassif (1993) on the feldspars. Salvi & Williams-Jones (1990, 1991, 1992) studied fluid inclusions from the Strange Lake complex. A model for the chemical evolution of the magmas was proposed by Boily & Williams-Jones (1994).

The geological map of the Strange Lake complex (Fig. 1) is based on field studies and description of drill cores by Miller (1986). The early units are dominantly hypersolvus, with minor areas of transsolvus granite. On a microscopic scale, the feldspars of these rocks are perthite with local rims or interstitial patches of albite and K-feldspar. The temporally intermediate rocks occupy the northern and western portions of the complex. These granites are transsolvus to subsolvus, distinguished by perthite phenocrysts in a two-feldspar groundmass or by the presence of two primary feldspars without perthite phenocrysts. The youngest rocks of the complex have extremely limited outcrop and are known mostly from drill core. Geochemically, these granites show high concentrations of rare elements such as Y, Nb, Zr, and Be (Miller 1988) and correspondingly high concentrations of minerals such as elpidite, pyrochlore and several rare minerals of Y and Be. These granites are all subsolvus.

The distribution of samples examined is illustrated in Figure 1. The latest-intruded granite and its derived pegmatite–aplite dykes (unit 4 in Fig. 1) were extensively studied through exploration drilling and examination of thin sections [see Birkett *et al.* (1992) for geological maps and sections of the central portion of the pluton]. Of the Ti-bearing minerals considered here, only amphibole, pyroxene, pyrochlore and titanite pseudomorphous after a tabular precursor mineral have been recognized in the central portion of the complex, and thus the details of sample distribution are not reported in Figure 1.

TABLE 1. ANALYTICAL CONDITIONS AND STANDARDS, ELECTRON-MICROPROBE ANALYSES

	Geological Survey of Canada (Ottawa, symbol *O*)		Harvard University (Cambridge, symbol *H*)
	Standards	D	Standards
Si	quartz	0.02	enstatite
Ti	rutile	0.04	rutile
Zr	zircon	0.2	zircon
Sn	cassiterite	0.2	cassiterite
Nb	niobium	0.2	Nb_2O_5
Al	corundum	0.02	kyanite
Fe	magnetite	0.07	fayalite
Mn	rhodonite	0.05	rhodonite
Mg	periclase	0.02	enstatite
Ca	wollastonite	0.04	anorthite
Zn	sphalerite	0.2	ZnO
Ba	sanbornite	0.2	celsian
Na	NaCl	0.03	albite
K	KBr	0.05	microcline
F	LiF	0.01	Fluor-biotite
La	LaB_6	0.2	not sought

Ce, Pr, Nd, and Eu were standardized to fluorides (*e.g.* CeF_3)
Sm, Gd, Tb, Dy, Ho, Er, Yb, Lu and Y were individually standardized to metals
Typical limits of detection for lanthanides were 0.2 to 0.3 except for Y (0.09)
In all Tables "-" indicates not analysed, n.d. not detected.
Analytical conditions 15 kV 10 or 30 nA, depending on the element sought.
Data reduction, Ottawa, by a modified PAP program (Pouchou & Pichoir, 1985); Harvard by a Bence-Albee proceedure (Sandia Laboratories) modified by D. Lange.
D: estimated limit of detection (weight %)

Analytical methods

Mineral compositions were determined by wavelength-dispersion electron-probe microanalysis using Cameca SX50 electron microprobes at Harvard University in Cambridge, and at the Geological Survey of Canada in Ottawa. Fe^{2+} and Fe^{3+} are calculated from total Fe by recalculation to accommodate charge balance and stoichiometry. The method is explained in detail for each mineral. In Tables 2 – 9, the symbol "–" indicates that the element was *not sought*; the symbol "n.d." indicates that the element was *not detected.* Inferred concentrations are presented in parentheses (*i.e.*, Fe^{3+}, Li). The standards used, estimated precision and detection limits are given in Table 1.

PETROGRAPHY OF THE Ti-BEARING MINERALS

The rocks described here are all granitic. Abundant quartz, one or two feldspars, fluorite and pyrochlore are present in all samples examined. The earliest-crystallized Ti-bearing minerals are bafertisite, ilmenite, aenigmatite, and astrophyllite. These were followed, in some cases through reaction, by neptunite, arfvedsonite, and aegirine. Narsarsukite and titanite pseudomorphous after narsarsukite formed under late igneous to subsolidus conditions (Fig. 2). In a few samples, Ti-bearing minerals were not identified. Such rocks have anomalously high amounts of fine-grained

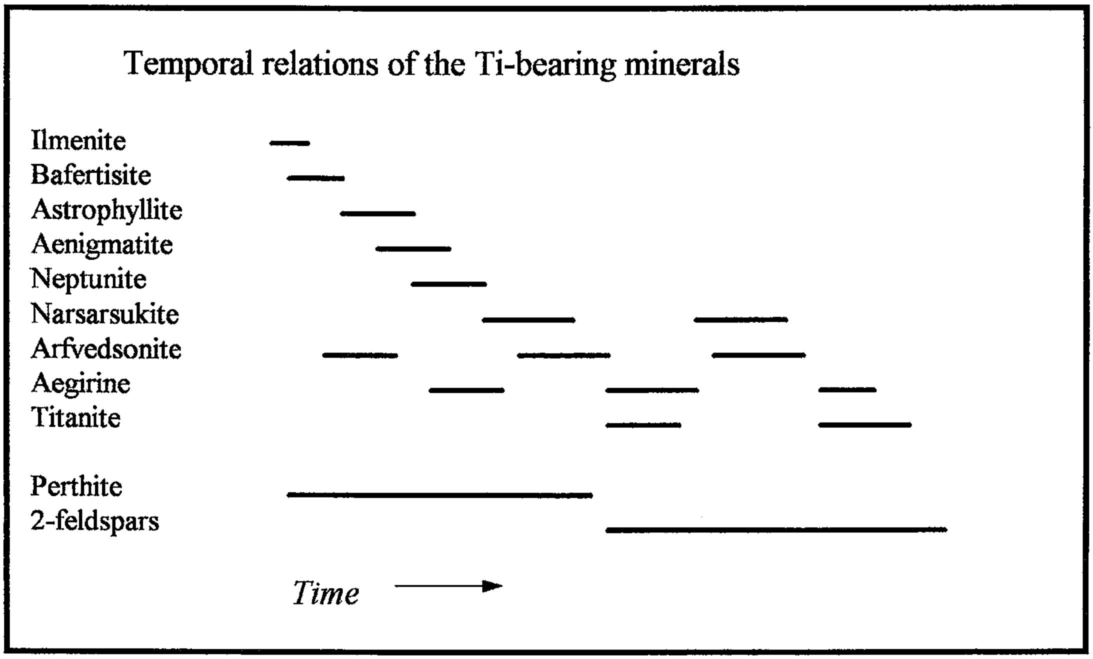

FIG. 2. Temporal relations among the Ti-bearing minerals at Strange Lake.

dark amphibole or pyroxene, which are sufficiently abundant to incorporate all the available Ti in solid solution.

Ilmenite forms equant, rounded grains invariably armored in other Ti–Fe-silicates. Ilmenite occurs surrounded by a rim of bafertisite, by astrophyllite included within aenigmatite, or simply by aenigmatite. In general, the ilmenite and rim of Ti–Fe-silicate are themselves enclosed in amphibole; relics enclosed in aenigmatite are less common. In only one sample was ilmenite, rimmed by astrophyllite, found between amphibole and feldspar; in one other sample, ilmenite occurs within quartz.

Astrophyllite occurs in four principal habits at Strange Lake: small plates enclosed in feldspar, large independent subhedral to ragged crystals (Fig. 3B), irregular corroded relics enclosed in amphibole (Fig. 3A), and masses of crystals surrounding and embaying aenigmatite or ilmenite. The occurrence of small plates of astrophyllite within feldspar (Fig. 3C), associated with small crystals of arfvedsonite, indicates the approximately simultaneous crystallization of these three minerals.

Aenigmatite forms elongate crystals, equant spongy grains or elongate grains cementing perthitic feldspar. Distinguished by very deep red absorption and marked pleochroism, lamellar twinning in a few examples, and patchy zoning, aenigmatite is associated with perthitic feldspar, fluorite, zircon, vlasovite and quartz. Commonly, the aenigmatite shows the results of later reactions and is partially enclosed within amphibole (Fig. 3D) or neptunite (Fig. 4C), or converted to astrophyllite along grain margins and cracks.

Neptunite, a relatively common accessory, appears as red to red-orange irregular or equant grains. In rare cases, it occurs as subhedral to euhedral crystals (Fig. 4D). In some cases, neptunite is rimmed or veined by arfvedsonite or by astrophyllite or, locally, by aegirine. Neptunite in other cases rims or replaces aenigmatite (Fig. 4C) and, locally, astrophyllite. In one sample, neptunite forms equant grains interstitial to perthite and thus may be in stable coexistence with nearby narsarsukite and arfvedsonite.

Narsarsukite and *titanite* pseudomorphic after narsarsukite are found throughout the Strange Lake pluton. High relief, second-order birefringence and a strong tendency to idiomorphism aid in identifying narsarsukite. In the northern and central portions of the complex, the tabular pseudomorphs of titanite occcur to the exclusion of the other Ti-rich accessory phases. Narsarsukite occurs locally as poikilitic crystals, up to several millimeters in maximum dimension, in the southern portions of the pluton. It also forms early, equant grains interstitial to feldspars and quartz (Fig. 4B). In some samples, crystals of narsarsukite (in places now replaced by titanite) occur within fine-

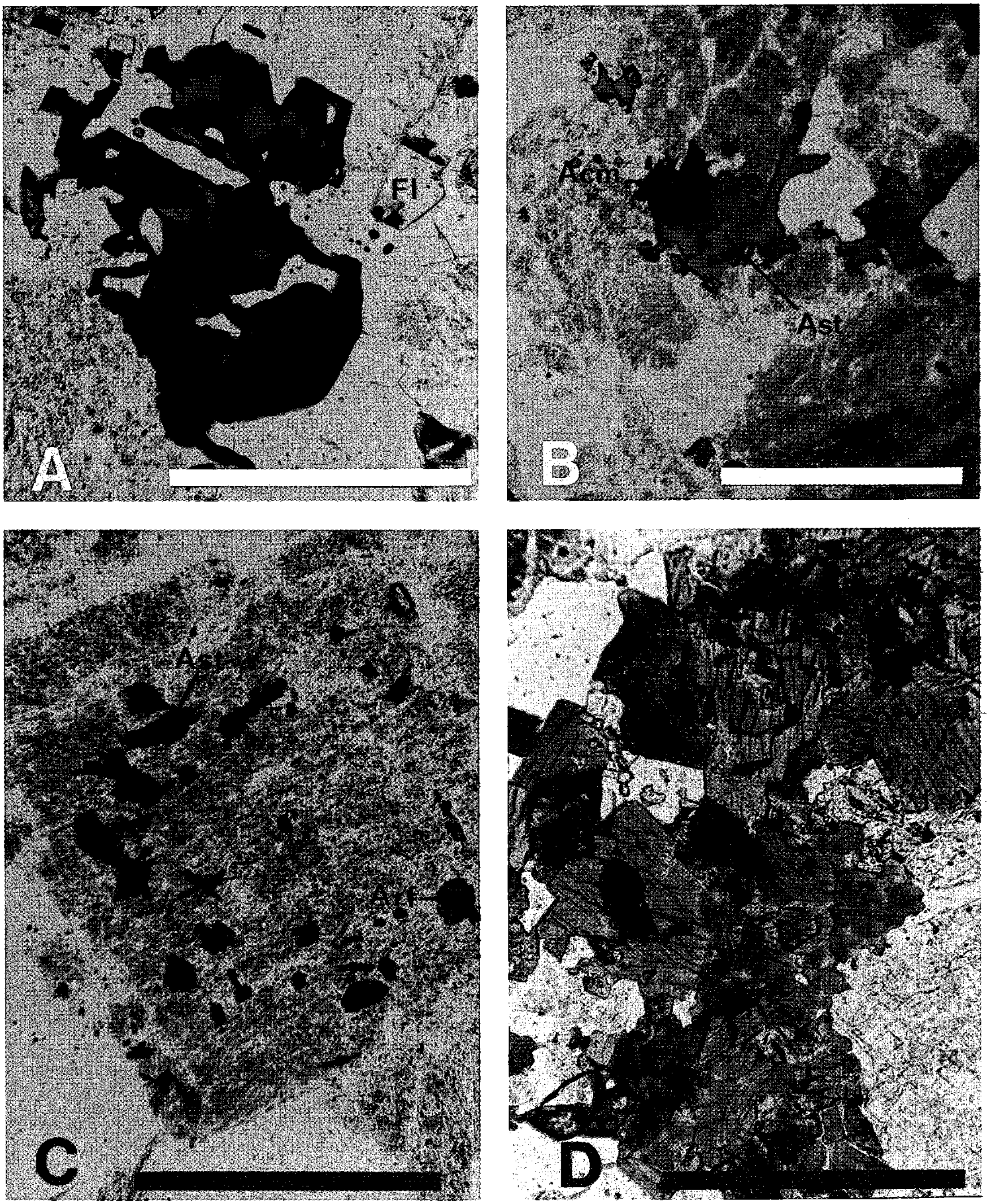

FIG. 3. Textural relations of astrophyllite and aenigmatite. A. Astrophyllite embayed and replaced by amphibole. Less obvious are dark relics of aenigmatite in the same amphibole. Associated minerals are perthitic feldspar, quartz, and fluorite. Scale bar indicates 500 μm, plane light. B. Astrophyllite in contact with sodic pyroxene. Associated minerals are perthitic feldspar, quartz, sodic amphibole and fluorite. Scale bar 1 mm, plane light. C. Inclusions of equant amphibole and laths of astrophyllite in perthitic feldspar. The zonal distribution of the inclusions indicates that they were included in the feldspar during its crystallization. Scale bar 500 μm, plane light. D. Relics of aenigmatite in sodic amphibole. Scale bar represents 500 μm, plane light.

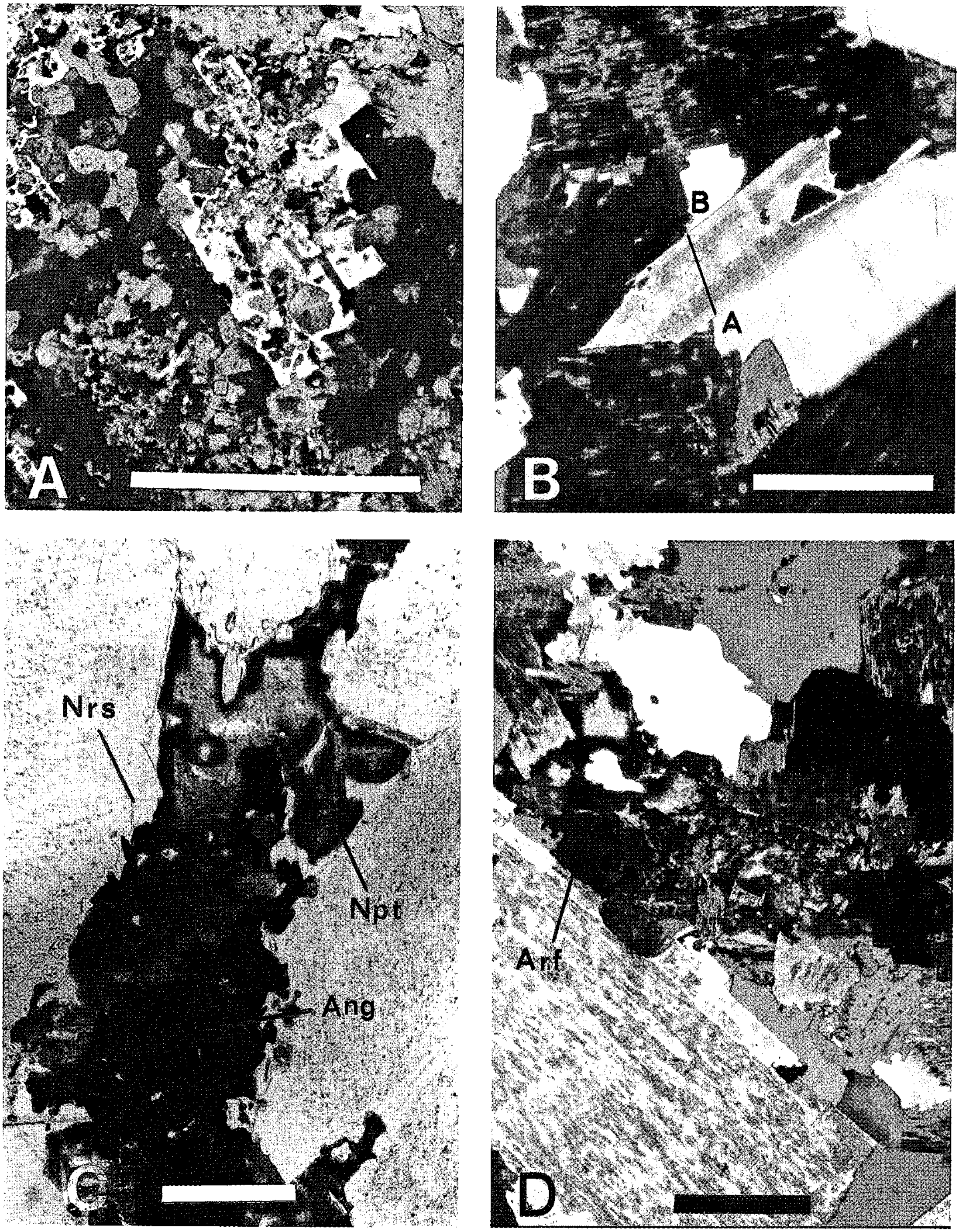

grained granitic inclusions (Fig. 5) and cross the contacts with the host granite; these crystals may have formed later, in the subsolidus regime. Elsewhere, especially in the southern portion of the complex, narsarsukite forms poikilitic grains cementing earlier-formed minerals of the rocks (Fig. 4A) associated with quartz, sodic amphibole, fluorite, hilairite, K-feldspar, and albite. These occurrences may have formed from a

FIG. 4. Textural relations of narsarsukite and neptunite. A. Subhedral, poikilitic crystal of narsarsukite with fine-grained, subhedral sodic amphibole. All of the narsarsukite in the image has the same optical orientation and is interpreted as a single crystal. Associated minerals are quartz, K-feldspar, albite, fluorite, and hilairite. Scale bar represents 500 μm; crossed polarizers. B. Optically and chemically zoned crystal of narsarsukite, in optical continuity with the narsarsukite at the lower left of the photograph. The crystal shows a core (yellow) separated from a mantle (red) by a zone of micro-inclusions, and a thin rim (yellow). Associated minerals are perthitic feldspar, quartz, and sodic pyroxene (below the narsarsukite), with a small core of sodic amphibole. Scale bar represents 500 μm, crossed polarizers. C. Colorless narsarsukite as a thin film surrounding neptunite. Included within the neptunite are relics of aenigmatite with common optical orientation, small grains of astrophyllite and sodic amphibole. Locally, the neptunite is rimmed by sodic amphibole (upper portion of the image). Associated minerals are quartz, fluorite and perthitic feldspar. Scale bar indicates 1 mm; plane light. D. Sodic amphibole (at extinction) is veined and surrounded by neptunite. The sodic amphibole is also locally embayed by sodic pyroxene (lower portion of the image). Associated minerals are perthitic feldspar, quartz and fluorite. Scale bar indicates 1 mm, crossed polarizers.

←

residual melt or even a postmagmatic fluid enriched in Ti, Na and F. Typically, these crystals of narsarsukite show anomalously low birefringence and relief. A thin rim of narsarsukite, surrounding embayed earlier-formed Ti-bearing minerals, is locally present (Fig. 4B). In the northern and central portions of the pluton, in the more evolved rocks, the narsarsukite, precursor to the tabular pseudomorphs of titanite, occurs as equant grains formed during the primary crystallization of the rocks. In the dyke that forms the principal rare-metals deposit at Strange Lake, the primary crystals of narsarsukite (now replaced by titanite) share a flow alignment with other elongate grains (albite, monazite, and one or more Zr-bearing minerals). Local partial replacement confirms that titanite is secondary after narsarsukite.

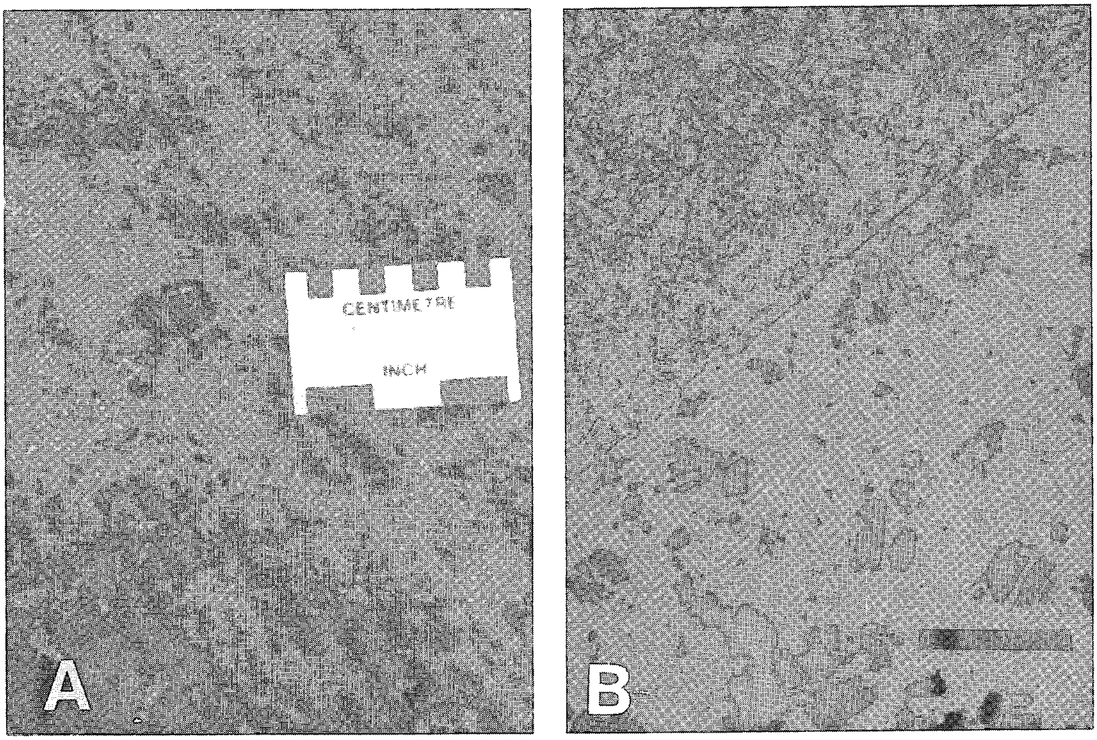

FIG. 5. Textural relations of narsarsukite. A. Development of narsarsukite porphyroblasts (light-colored laths) in inclusions of fine-grained alkali granite. Similar porphyroblasts are also present in the surrounding medium-grained granite. Locally, the porphyroblasts cross the contacts of the inclusions. B. A poikilitic grain of narsarsukite (upper portion of the image, high relief). Within the poikiloblast, the sodic amphibole in the rock matrix has disappeared, as has most of the quartz, leaving feldspar and fluorite. Scale bar is 500 μm, plane light.

CHEMICAL COMPOSITION OF THE TI-BEARING MINERALS

Aenigmatite

Aenigmatite (simplified formula $Na_2Fe^{2+}_5TiO_2[Si_6O_{18}]$) is a widespread minor constituent of the least-evolved rocks at Strange Lake. It is the most common member of the aenigmatite group of general formula $A_2B_6T_6O_{20}$, where ^{VIII}A cations include Na and Ca, ^{VI}B cations are Fe^{2+}, Fe^{3+}, Mg, Mn, Al, and Ti (among others), and ^{IV}T cations include Si, Al, B, and Be, as discussed by Burt (1994). Electron-microprobe analyses of samples from Strange Lake (Table 2) indicate solid solution toward wilkinsonite $Na_2Fe^{2+}_4Fe^{3+}_2Si_6O_{20}$ (Duggan 1990) and only minor solid solution toward dorrite $Ca_2(Mg_2Fe^{3+}_4)(Al_4Si_2)O_{20}$ (Cosca *et al.* 1988). Concentrations of Nb, Zr, Sn and Zn are low. Calculation of Fe^{3+} on the basis of 20 oxygen equivalents and 12 cations, excluding Na, yields good fits to the electron-microprobe data when the entry of Nb is modeled by $Ti_2[NbFe^{3+}]_{-1}$. Other substitutions involving Nb also may model the data adequately, although the range of Nb concentrations is not sufficiently large to test these possibilities. Other substitutions involving Nb in minerals have been discussed by Černý & Ercit (1989). The distributions of data points fit a substitution modeled by $(R^{4+}R^{2+})R^{3+}_{-2}$ (Fig. 6) when the contents of Ca and Nb are compensated. The excess of Ti + 2Nb over 1 cation per 20 oxygen atoms and Si less than 6 atoms (Fig. 7) indicate that incorporation of Nb and trivalent cations involve several sites in the mineral.

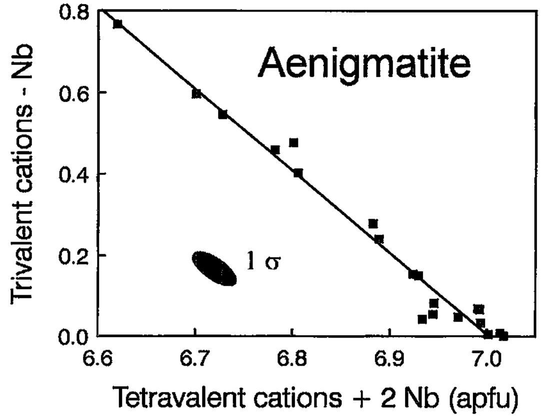

FIG. 6. Inferred proportions numbers of trivalent and tetravalent cations in aenigmatite (based on 20 atoms of oxygen) after the entry of niobium is accounted for by the substitution $Ti_2(NbFe^{3+})_{-1}$. The line of slope –2 represents the results of the ideal substitution $R^{4+}R^{2+}(R^{3+})_{-2}$.

TABLE 2. AENIGMATITE COMPOSITIONS, STRANGE LAKE GRANITE

wt.%	*H* 016–16	*O* 016–17	*O* 015–6–1	*O* 017–13	*O* –15XA11
SiO_2	41.96	42.17	42.47	40.60	41.36
ZrO_2	0.08	0.02	0.09	nd	nd
TiO_2	9.13	8.99	9.27	8.92	8.86
SnO_2	0.02	0.08	0.09	0.06	0.01
Nb_2O_5	0.09	0.09	0.19	0.24	nd
Al_2O_3	0.36	0.23	0.08	0.17	0.03
Ce_2O_3	–	–	0.01	nd	0.41
Y_2O_3	–	–	nd	nd	nd
(Fe_2O_3)	0	0	0	2.08	0
FeO	40.12	39.43	40.23	38.90	39.65
MnO	0.94	0.94	1.28	1.18	1.11
MgO	0.01	0.03	0.01	0.03	0.03
BaO	0.09	0.06	0.01	0.03	nd
CaO	0.21	0.12	0.03	0.08	0.01
ZnO	0.09	0.04	0.35	0.17	nd
Na_2O	8.03	8.06	7.38	6.83	6.90
K_2O	0.02	0.01	0.03	0.04	nd
F	nd	0.08	nd	nd	nd
Total	101.15	100.35	101.52	99.34	98.37
–O≡F	0	0.03	0	0	0
Sum	101.15	100.32	101.52	99.34	98.37
cations					
Si	5.95	6.01	6.00	5.88	6.03
Zr	0.01	0.00	0.01	0	0
Ti	0.97	0.96	0.98	0.97	0.97
Sn	0.00	0.01	0.01	0.00	0.00
Nb	0.01	0.01	0.01	0.02	0
Al	0.06	0.04	0.01	0.03	0.01
Ce	–	–	0.00	0	0.02
Y	–	–	0	0	0
(Fe^{3+})	0	0	0	0.23	0
Fe^{2+}	4.76	4.70	4.75	4.71	4.84
Mn	0.11	0.11	0.15	0.15	0.14
Mg	0.00	0.01	0.00	0.01	0.01
Ba	0.01	0.00	0.00	0.00	0
Ca	0.03	0.02	0.00	0.01	0.00
Zn	0.01	0.00	0.04	0.02	0
Na	2.21	2.23	2.02	1.92	1.95
K	0.00	0.00	0.01	0.01	0
F	0	0.04	0	0	0

Electron–microprobe analyses of aenigmatite. Cations are calculated on a basis of 20 oxygen atoms and 12 **B** and **T** cations as discussed in the text. (Fe_2O_3) calculated from stoichiometry.

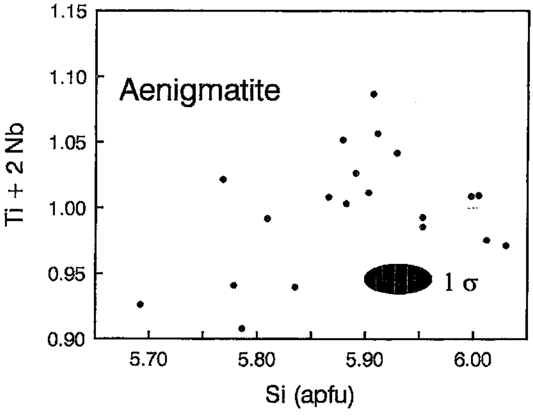

FIG. 7. Proportions of atoms of Si *versus* Ti + 2 Nb (*apfu*) in aenigmatite (based on 20 atoms of oxygen). The ideal composition of aenigmatite is indicated by the cross.

TABLE 3. ASTROPHYLLITE AND NIOBOPHYLLITE COMPOSITIONS

WT.%	1	2	3	4	5	6	7	8	9
	5617-5	5617-7	5663-6	5654-3	5879-A9	H31-6	5860-2	Nio1	Nio7
SiO_2	35.84	35.92	36.73	35.93	35.69	34.93	36.42	33.63	33.49
ZrO_2	0.67	1.40	0.15	1.38	0.24	1.11	1.51	0.24	nd
TiO_2	10.46	9.48	11.99	9.15	11.32	10.05	10.60	2.69	2.70
SnO_2	0.17	0.27	nd	0.01	0.10	0.18	nd	0.18	0.09
Nb_2O_5	1.76	2.02	0.18	3.47	0.37	1.21	0.15	10.23	10.32
Al_2O_3	0.34	0.18	0.40	0.23	0.18	0.26	0.07	1.20	1.40
Ce_2O_3	-	-	-	-	nd	nd	0.15	0.19	nd
Y_2O_3	-	-	-	-	nd	nd	nd	nd	nd
(Fe_2O_3)	7.26	8.96	1.90	14.04	2.40	1.28	5.94	1.47	1.45
FeO	26.97	24.85	33.13	19.84	30.60	32.62	29.14	25.28	24.87
MnO	1.82	1.96	1.37	1.78	2.47	2.31	0.93	8.81	8.66
MgO	0.03	0.03	0.07	0.04	0.05	0.03	0.20	0.20	0.21
BaO	0.31	0.12	0.14	0.20	0.52	0.26	0.11	2.12	nd
CaO	0.18	0.20	0.31	0.75	0.38	0.28	0.16	0.93	0.65
ZnO	0.16	0.21	0.10	0.21	0.65	0.55	0.11	0.13	0.28
Na_2O	3.65	3.66	3.54	3.17	3.30	3.02	3.57	0.88	1.26
K_2O	4.92	5.18	5.47	5.43	4.96	5.45	5.16	1.87	2.24
F	1.13	0.91	1.43	1.38	0.93	0.78	1.52	nd	nd
Total	95.67	95.36	96.91	97.01	94.30	94.51	95.59	89.87	87.62
-O≡F	0.48	0.38	0.60	0.58	0.39	0.33	0.64	0.00	0.00
Sum	95.19	94.97	96.31	96.43	93.91	94.18	94.95	89.87	87.62
cations									
Si	7.84	7.86	7.99	7.71	7.98	7.90	8.00	7.99	8.02
Zr	0.07	0.15	0.02	0.14	0.03	0.12	0.16	0.09	0
Ti	1.72	1.56	1.96	1.48	1.90	1.71	1.75	0.48	0.48
Sn	0.02	0.03	0	0.00	0.01	0.02	0	0.01	0
Nb	0.17	0.20	0.02	0.34	0.04	0.12	0.02	1.09	1.11
Al	0.09	0.05	0.10	0.06	0.05	0.07	0.02	0.33	0.39
Ce	-	-	-	-	0	0	0.01	0.02	0
Y	-	-	-	-	0	0	0	0	0
(Fe^{3+})	1.20	1.48	0.31	2.27	0.40	0.22	0.98	0.26	0.26
Fe^{2+}	4.94	4.55	6.03	3.56	5.72	6.17	5.35	5.02	4.98
Mn	0.34	0.36	0.25	0.32	0.47	0.44	0.17	1.77	1.75
Mg	0.01	0.01	0.02	0.01	0.02	0.01	0.07	0.07	0.07
Ba	0.03	0.01	0.01	0.02	0.05	0.02	0.01	0.19	0
Ca	0.04	0.05	0.07	0.17	0.09	0.07	0.04	0.23	0.16
Zn	0.03	0.03	0.02	0.03	0.11	0.09	0.02	0.02	0.04
Na	1.55	1.55	1.49	1.32	1.43	1.32	1.52	0.40	0.58
K	1.37	1.45	1.52	1.49	1.42	1.57	1.45	0.56	0.68
F	0.78	0.63	0.98	0.94	0.66	0.56	1.06	0	0

Electron-microprobe analyses of astrophyllite and niobophyllite (columns 8 & 9) calculated on an anhydrous basis of 28.5 oxygen atoms.

Astrophyllite

Astrophyllite, a silicate of simplified formula $(Na,K)_3Fe_7Ti_2Si_8(O,OH)_{31}$, is a common accessory mineral in the least evolved to moderately evolved rocks at Strange Lake. Following the terminology of Layne *et al.* (1982), the formula can be expressed as $W_3X_7Y_2Z_8A_{31}$, where W includes the 10- to 13-coordinated cations Na, K, Ca and Cs, X represents the eight-coordinated cations Fe^{2+}, Mn, Mg, Zn and Li, Y represents the octahedrally coordinated cations Ti, Zr, Nb, Sn, Fe^{3+}, and Z, the tetrahedrally coordinated cations Si, Al, and Fe^{3+}. Electron-probe microanalyses of astrophyllite from Strange Lake (Table 3) indicate variable solid-solution toward the end members kupletskite (Mn) and zircophyllite (Zr), and toward a Nb analogue of astrophyllite (but a phase that is distinct from niobophyllite). The principal substitutions recorded from Strange Lake are Zr (0.5 to 3 wt.% ZrO_2), Nb (0.5 to 2 wt.% Nb_2O_5), and Al (0.5 to 1.5 wt.% Al_2O_3).

Abdel-Rahman (1992) suggested that Nb enters the astrophyllite structure through the substitution $Nb^{5+} = Ti^{4+}$ + vacancy. There are two mechanisms compatible with Abdel-Rahman's (1992) formulation: $[X]Nb_2(Fe^{2+}Ti_2)_{-1}$ and $[W]Nb(NaTi)_{-1}$, where Na includes Na, K, Cs, *etc.*, and where $[X]$ indicates a vacancy in the site of eight-coordinated cations, following Burt (1989). These substitutions both predict a 1:1 negative correlation between Nb and Ti in astrophyllite. The situation is complicated, however, by the presence of other tetravalent cations that may

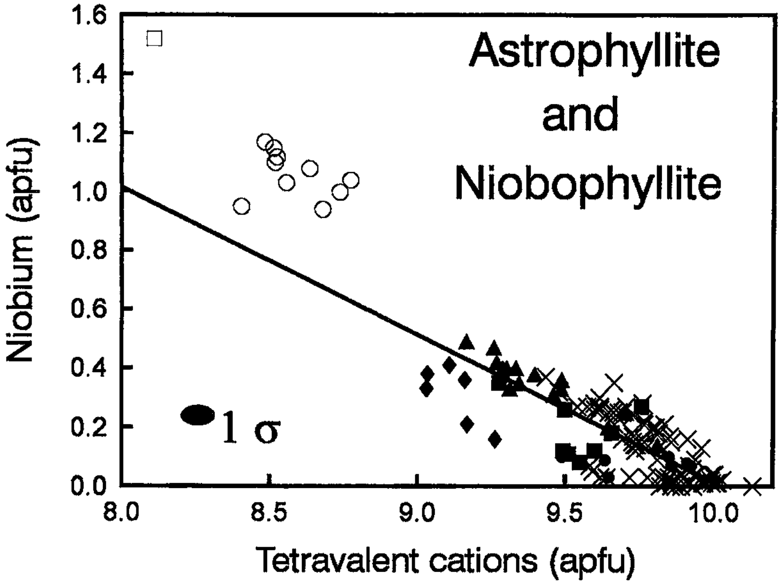

FIG. 8 Proportions of tetravalent cations *versus* Nb atoms (based on 28.5 oxygen atoms) in astrophyllite and niobophyllite. The line indicates a slope of –0.5 equivalent to a substitution of the form $R_2^{4+}(\mathrm{NbFe}^{3+})_{-1}$. Symbols: × astrophyllite, this study, ○: niobophyllite, this study, ■ Abdel-Rahman (1992), ● Macdonald & Saunders (1973), □ Nickel *et al.* (1964), ▲ Martin (1975), ◆ Layne & Rucklidge (1982).

substitute for Ti (*e.g.*, Zr and Sn). Finally, analyses of astrophyllite commonly report less than the ideal 8 atoms per formula units of Si (*apfu*). Thus some trivalent or tetravalent cations may be assigned to fill the requirement for 8 Si. Consequently, we test the Nb substitution in astrophyllite by examining the correlation between the sum of tetravalent cations (R^{4+}) and Nb atoms (Fig. 8). Examination of our data and other published compositions, either separately or combined, indicates that the correlation bewteen R^{4+} and Nb is near –0.5. Calculations with various ferrous–ferric ratios have only a minor effect on the calculated correlations, and cannot be an important factor in astrophyllite because all studies to date have shown that iron in the mineral is dominantly Fe^{2+}. Thus the substitution of Nb into astrophyllite is better modeled by $\mathrm{Nb}^{5+} = 2R^{4+}$ ± other atoms to maintain charge balance. There are no significant correlations between the sums of monovalent cations or the sums of divalent cations and Nb in available compositions of astrophyllite, but there is a negative correlation between levels of Si and Nb. If the difference of total cations from the ideal 20 cations per 28.5 oxygen atoms is taken as an approximate measure of vacancies, no significant correlation exists between Nb substitution and vacancies. The presence of excess H in interlayer sites cannot be tested with the available data. A straightforward substitution suggested for the incorporation of Nb is $\mathrm{Nb}R^{3+}(R^{4+})_{-2}$. This substitution, common in the perovskite group, for example, also leads to predictions of the R^{3+} of the mineral, and thus leads to a model for ferric iron incorporation in astrophyllite.

The substitution $\mathrm{Nb}R^{3+}(R^{4+})_{-2}$ allows a lower limit to be placed on the R^{3+} content of astrophyllite. The number of cations calculated after application of the Nb model, however, should still approximate an astrophyllite formula in terms of the numbers of other cations. Thus the formula should yield Si = 8 or less, and R^{4+} + 2 Nb = 10 or less. After modeling Nb in astrophyllite, there commonly remains an excess of atoms (in the total R^{4+} + 2 Nb), and a second substitution must be invoked. The substitution $R_2^{3+}(R^{4+}R^{2+})_{-1}$ is commonly computed to limit the proportion of R^{4+} cations to a total based on the mineral's stoichiometry.

Relationship between astrophyllite and niobophyllite

Niobophyllite, $(\mathrm{K,Na})_3(\mathrm{Fe}^{2+},\mathrm{Mn})_6(\mathrm{Nb,Ti})_2\mathrm{Si}_8(\mathrm{O,OH,F})_{31}$, was defined by Nickel *et al.* (1964) and has been considered an end member of a solid solution with astrophyllite (Nickel *et al.* 1964, Macdonald & Saunders 1973, Abdel-Rahman 1992). The substitution relating astrophyllite and niobophyllite can be expressed as $[X]Nb_2(Ti_2Fe^{2+})_{-1}$. No astrophyllite analyzed to date by Abdel-Rahman (1992), Macdonald & Saunders (1973), Layne *et al.* (1982) or in the present study shows a systematic deficiency in R^{2+} cations that would indicate solid solution toward the niobophyllite composition of Nickel *et al.* (1964). To investigate these observations further, new electron-probe microanalyses of "niobophyllite" from Seal Lake, Labrador, were completed. Without a more definite formula for niobophyllite, Fe^{3+} in the results of the new microprobe analyses of Seal Lake material has been calculated at 5% of total iron present. These data, included in Table 3 and Figure 8, do not match well with the single published composition of niobophyllite and, furthermore, do not fall on the trend defined by astrophyllite compositions. The newly determined compositions of Seal Lake niobophyllite do not show a deficiency in R^{2+} cations but are deficient in Na and K (Table 3). The relationship between R^{4+} and Nb (Fig. 8) suggests a range of Ti:Nb values rather than a simple substitution. The deficiency in interlayer cations suggests that Nb may enter this phase by a substitution such as $[W]Nb(TiNa)_{-1}$. Another possibility is to model the incorporation of Nb in "niobophyllite" from Seal Lake by $Ti_3[Fe^{2+}Nb_2]_{-1}$, as suggested by Larsen *et al.* (1992) for the entry of Nb in the mineral lorenzenite ($Na_2Ti_2Si_2O_9$). The data, however, do not support the presence of "excess" R^{2+} in this phase, and the substitution would require the entry of Fe^{2+} (ionic radius 0.76 Å) into a site normally occupied by Ti^{4+} (ionic radius 0.68 Å).

The data available indicate that more than one mechanism of Nb incorporation may be involved among minerals in the astrophyllite group, that niobophyllite is not the only possible Nb analogue of astrophyllite, and that further examination of the type material for niobophyllite and other members of the astophyllite group is required.

TABLE 4. BAFERTISITE COMPOSITIONS, STRANGE LAKE GRANITE

	H NF5663–4	*H* NF5663–5	*O* NF5663–18	*O* NF5663–A	*O* H39–1	*O* H39–2
SiO_2	24.22	24.33	23.88	24.11	26.24	21.83
ZrO_2	0.08	0.19	0.42	0.12	nd	0.12
TiO_2	16.80	15.84	14.47	15.08	20.61	29.84
SnO_2	nd	nd	0.08	0.08	0.08	0.07
Nb_2O_5	0.21	0.18	0.75	0.20	0.51	0.88
Al_2O_3	0.08	0.08	0.19	0.29	0.46	0.42
La_2O_3	–	–	–	0.18	–	–
Ce_2O_3	–	–	nd	1.71	2.97	3.06
Nd_2O_3	–	–	–	0.50	–	–
Sm_2O_3	–	–	–	nd	–	–
Gd_2O_3	–	–	–	0.09	–	–
Y_2O_3	–	–	nd	nd	nd	nd
(Fe_2O_3)	0	0	0	0	0	0
FeO	25.89	25.38	25.17	29.25	12.78	10.30
MnO	1.43	1.39	1.73	1.40	0.92	0.65
MgO	0.00	0.00	0.04	0.11	nd	0.02
BaO	28.47	28.87	28.81	24.15	25.21	28.13
CaO	0.02	0.04	0.06	0.06	0.23	0.16
ZnO	nd	nd	0.06	0.16	0.31	0.14
Na_2O	0.08	0.10	0.23	0.65	0.41	0.48
K_2O	0.13	0.15	0.16	1.52	0.84	0.51
F	5.38	5.60	5.16	2.59	2.25	1.96
Total	102.79	102.15	101.21	102.25	93.82	98.57
–O≡F	2.27	2.36	2.17	1.09	0.95	0.83
Sum	100.52	99.79	99.04	101.16	92.87	97.74
cations						
Si	2.01	2.05	2.04	1.97	11.52	9.24
Zr	0.00	0.01	0.02	0.01	0	0.03
Ti	1.05	1.00	0.93	0.93	6.81	9.50
Sn	0	0	0.00	0.00	0.02	0.01
Nb	0.01	0.01	0.03	0.01	0.10	0.17
Al	0.01	0.01	0.02	0.03	0.24	0.21
La	–	–	–	0.01	–	–
Ce	–	–	0	0.05	0.48	0.47
Nd	–	–	–	0.02	–	–
Sm	–	–	–	0	–	–
Gd	–	–	–	0.00	–	–
Y	–	–	0	0	0	0
(Fe^{3+})	0	0	0	0	0	0
Fe^{2+}	1.80	1.79	1.80	2.00	4.69	3.65
Mn	0.10	0.10	0.13	0.10	0.34	0.23
Mg	0	0	0.01	0.01	0	0.01
Ba	0.93	0.95	0.96	0.77	4.34	4.66
Ca	0.00	0.00	0.01	0.01	0.11	0.07
Zn	0	0	0.00	0.01	0.10	0.04
Na	0.01	0.02	0.04	0.10	0.35	0.39
K	0.01	0.02	0.02	0.16	0.47	0.28
F	1.41	1.49	1.39	0.67	3.12	2.62

Electron–microprobe analyses of bafertisite and a bafertisite–like phase (analyses H39–1 and H39–2). Structural formulae of bafertisite are calculated to 9 oxygen atom equivalents, and of the bafertisite–like phase, to 48 oxygen atom equivalents.

Bafertisite, bafertisite-like phase

The occurrence and chemistry of the rare mineral bafertisite $[BaFe_2TiO(Si_2O_7)(OH,F)_2]$ and the Mn-analogue hejtmanite have been reviewed recently by Vrána *et al.* (1992). Other analytical data were reported for bafertisite and an unidentified bafertisite-like phase from North Carolina by Mauger (1983). At Strange Lake, a phase identified as bafertisite from its composition occurs as a thin rim mantling grains of ilmenite. Analytical data (Table 4) show substantial concentrations of the light rare-earth elements (up to 2 wt.% Ce_2O_3, not reported in studies of bafertisite from other localities), in addition to Nb concentrations of up to 0.5 wt.% Nb_2O_5 (similar to earlier reports). Spot analyses show that the rare earths are not distributed evenly throughout the mineral. Data are not available for all the rare-earth elements. A phase similar to bafertisite, but with higher Ti and Ce and lower Fe, has been analyzed (Table 4). It also occurs as a rim around ilmenite grains, and is referred to as a bafertisite-like mineral because of the similarities in occurrence, composition, and optical properties. This is not, however, the same phase as was analyzed by Mauger (1983). The low analytical totals suggest that it may be hydrous.

Ilmenite

Ilmenite has been identified in the Strange Lake peralkaline granites as minute grains rimmed by bafertisite or a similar phase, or by astrophyllite, and occluded in aenigmatite or amphibole. Chemically, the ilmenite is rich in Nb and Mn (Table 5) and thus linked to the composition of the host granite. In general, there is no correlation between levels of Ti and Ba in our analytical results, and the reported Ba in the ilmenite is thus not an analytical artifact. The association of

TABLE 5. ILMENITE COMPOSITIONS, STRANGE LAKE GRANITE

wt. %	*O*	*H*	*O*
	NF5633–A–7	NF5633–1	NF5879–A–2*
SiO_2	0.07	0.04	0.90
ZrO_2	nd	–	0.17
TiO_2	51.67	50.62	50.50
SnO_2	nd	–	nd
Nb_2O_5	0.66	1.24	0.73
Al_2O_3	0.04	0.11	0.02
Ce_2O_3	0.08	–	0.08
Y_2O_3	nd	–	nd
(Fe_2O_3)	0.99	0	0
FeO	43.72	42.16	40.35
MnO	2.82	2.91	5.17
MgO	0.01	nd	nd
BaO	0.42	–	1.30
CaO	0.05	–	0.08
ZnO	0.15	–	0.49
Na_2O	0.04	–	nd
K_2O	0.01	–	0.10
F	nd	–	nd
Total	100.73	97.08	99.89
Atoms			
Si	0.00	0.00	0.02
Zr	0	–	0.00
Ti	0.98	0.99	0.97
Sn	0	–	0
Nb	0.01	0.02	0.01
Al	0.00	0.00	0.00
Ce	0.00	–	0.00
Y	0	–	0
(Fe^{3+})	0.02	0	0
Fe^{2+}	0.92	0.92	0.86
Mn	0.06	0.06	0.11
Mg	0.00	0	0
Ba	0.00	–	0.01
Ca	0.00	–	0.00
Zn	0.00	–	0.01
Na	0.00	–	0
K	0.00	–	0.00
F	0	–	0
Total	2.00	1.99	2.00

Representative electron–microprobe analyses of ilmenite, calculated on a basis of three atoms of oxygen and two cations.

TABLE 6. NARSARSUKITE COMPOSITIONS

wt. %	Core 12	9	4	3	Rim 19	5638-2	56381 11
SiO_2	61.47	60.97	61.34	61.65	61.52	60.87	62.04
ZrO_2	0.54	1.27	2.77	1.86	0.92	2.21	1.03
TiO_2	12.54	12.31	13.06	12.70	11.79	12.39	13.03
SnO_2	0.17	0.16	0.15	0.29	0.16	0.23	0.05
Nb_2O_5	0.70	0.76	0.64	0.52	0.64	1.03	0.37
Al_2O_3	0.72	0.66	0.56	0.59	0.58	0.58	0.86
Ce_2O_3	0.04	0.24	nd	0.14	0.06	nd	nd
Y_2O_3	0.18	0.58	nd	nd	nd	0.29	nd
Fe_2O_3	4.97	5.35	4.71	5.69	5.80	3.76	5.98
MnO	-	-	-	-	-	-	-
MgO	nd	0.01	0.01	0.03	0.01	0.03	0.03
BaO	0.21	nd	0.16	0.16	0.37	0.42	0.85
CaO	nd	0.02	nd	0.01	0.03	nd	0.03
ZnO	-	-	-	-	-	nd	nd
Na_2O	15.39	14.93	14.81	15.13	14.96	15.09	14.59
K_2O	0.03	0.02	0.05	0.01	0.11	0.05	0.05
F	1.71	1.72	1.62	1.65	1.51	1.34	1.78
Total	98.67	99.00	99.88	100.43	98.46	98.29	100.69
-F≡O	0.72	0.72	0.68	0.69	0.64	0.56	0.75
Sum	97.95	98.27	99.20	99.74	97.83	97.72	99.94
Atoms							
Si	4.02	4.00	3.99	3.99	4.05	4.02	4.00
Zr	0.02	0.04	0.09	0.06	0.03	0.07	0.03
Ti	0.62	0.61	0.64	0.62	0.58	0.62	0.63
Sn	0.01	0.01	0.00	0.01	0.01	0.01	0.00
Nb	0.02	0.02	0.02	0.02	0.02	0.03	0.01
Al	0.06	0.05	0.04	0.05	0.05	0.05	0.07
Ce	0.00	0.01	0	0.00	0.00	0	0
Y	0.01	0.02	0	0	0	0.01	0
Fe^{3+}	0.25	0.26	0.23	0.28	0.29	0.19	0.29
Mn	-	-	-	-	-	-	-
Mg	0	0.00	0.00	0.00	0.00	0.00	0.00
Ba	0.01	0	0.00	0.00	0.01	0.01	0.02
Ca	0	0.00	0	0.00	0.00	0	0.00
Zn	-	-	-	-	-	-	-
Na	1.95	1.90	1.87	1.90	1.91	1.93	1.82
K	0.00	0.00	0.00	0.00	0.01	0.00	0.00
F	0.35	0.36	0.33	0.34	0.31	0.28	0.36

ilmenite with bafertisite suggests elevated Ba in the environment of crystallization. Ilmenite is a magmatic phase that was in a reaction relationship with the residual liquid as crystallization and cooling continued. Marsh (1975) has described ilmenite rimmed by astrophyllite in syenite.

Narsarsukite

Narsarsukite has recently been studied and a modified formula suggested by Wagner *et al.* (1991): $Na_2[(Ti,Zr)_{(1-x)}Fe^{3+}]O_{1-x}F_xSi_4O_{10}\cdot(0–\frac{1}{2})H_2O$. Narsarsukite at Strange Lake (Table 6) commonly displays a chemical zonation, revealed by variations in the birefringence of crystals (Fig. 4B). Traverses indicate that the zonation is due to changes in Zr concentration, with antithetical variation in Fe (Fig. 9). Minor but systematic zoning in Y also has been documented, whereas Nb does not show regular spatial variation. In contrast to the findings of Wagner *et al.* (1991) on narsarsukite from other localities, that from Strange Lake does not display systematic variation in the Ti content. The chemical zoning of Figure 9 is re-emphasized in Figure 10, where the Zr content is compared to the level of trivalent cations corrected for Nb substitution. It is apparent that the numbers of trivalent cations entering the structure of the mineral varied systematically throughout its crystallization, first decreasing then increasing. This change may be due to variations in F activity rather than the availability of trivalent cations (see below).

Mineral formulae were calculated on the basis of 11 (O + F), rather than on 7 cations as suggested by Wagner *et al.* (1991), because the Na site may not be completely filled, and calculations to a constant number of cations will obscure site-filling relationships. The results of analyses of narsarsukite (with all iron considered as Fe^{3+}) calculate to slightly more than

TABLE 6. – Continued

	5638-14	NF5633-D-11	NF5633-D-15	NF5633-D-17	NF5633-D-18
SiO_2	62.14	63.62	63.50	64.64	63.46
ZrO_2	0.83	1.11	1.87	0.32	0.55
TiO_2	12.13	12.52	11.91	12.27	12.74
SnO_2	0.07	0.04	0.10	0.12	0.09
Nb_2O_5	0.56	0.64	0.43	0.25	0.32
Al_2O_3	0.74	1.03	0.92	1.29	1.20
Ce_2O_3	0.08	0.14	0.22	0.02	0.19
Y_2O_3	-	-	-	-	-
Fe_2O_3	5.82	5.86	5.57	5.53	5.83
MnO	-	0.09	0.03	0.01	nd
MgO	0.01	0.04	0.02	0.02	0.01
BaO	0.21	0.06	0.17	nd	0.22
CaO	0.01	0.03	0.03	0.02	0.01
ZnO	-	0.06	nd	0.04	nd
Na_2O	15.19	15.43	14.73	15.07	14.55
K_2O	nd	0.23	0.11	0.06	0.06
F	1.82	2.26	2.00	1.93	2.02
Total	99.61	103.16	101.61	101.59	101.25
-F≡O	0.77	0.95	0.84	0.81	0.85
Sum	98.85	102.21	100.77	100.78	100.40
Si	4.03	3.99	4.04	4.07	4.03
Zr	0.03	0.03	0.06	0.01	0.02
Ti	0.59	0.59	0.57	0.58	0.61
Sn	0.00	0.00	0.00	0.00	0.00
Nb	0.02	0.02	0.01	0.01	0.01
Al	0.06	0.08	0.07	0.10	0.09
Ce	0.00	0.00	0.01	0	0.00
Y	-	-	-	-	-
Fe^{3+}	0.28	0.28	0.27	0.26	0.28
Mn	0	0.01	0.00	0.00	0
Mg	0.00	0.00	0.00	0.00	0.00
Ba	0.01	0.00	0.00	0	0.01
Ca	0.00	0.00	0.00	0.00	0.00
Zn	0	0.00	0	0.00	0
Na	1.91	1.88	1.82	1.84	1.79
K	0	0.02	0.01	0.01	0.01
F	0.37	0.45	0.40	0.38	0.41

Electron-microprobe analyses of narsarsukite. Analyses labelled from core to rim are from the profile A B of Figure 5B. All iron is reported as Fe^{3+}. All analyses reported here were done in Ottawa.

the ideal 5 cations, exclusive of the Na site, so there is thus no basis for calculations with some iron expressed as Fe^{2+}. Nb incorporation is modeled as $R^{4+}_2(NbR^{3+})_{-1}$. Proportions of R^{4+} and R^{3+} cations covary, with a correlation of slope near –1 (Fig. 11). The relationships of F with R^{3+} and R^{4+} cations approximate lines of slope 1 and –1, respectively (Figs. 12, 13). The substitution scheme proposed by Wagner *et al.* (1991), $R^{4+}O(R^{3+}F)_{-1}$, thus seems dominant. However, it leaves much of the F unaccounted for, with the majority of the data points plotting above the line on Figure 12. This may be an analytical artifact. Wagner *et al.* (1991) attributed this excess to the presence of divalent cations assumed to enter the structure by a substitution $R^{4+}O_2(R^{2+}F_2)_{-1}$. Since the sum of cations is already high, and recalculation with more Fe^{2+} will lead to an apparent increase in this sum, it is unlikely that this scheme is significant. A moderate correlation exists between the "excess" F and vacancies in the Na site (which are calculated as the difference in charge of {Na + K + Ba + Ca} from 2+). Analytical data from this study and from Wagner *et al.* (1991) commonly show a small excess number of atoms in the Si and Ti sites. This may also be an analytical artifact, or it may indicate that other atoms (such as Ti and Fe^{3+} or Fe^{2+}) also can occupy the Na sites (Fe^{2+} being much more likely than the others). The present dataset does not resolve the possible entry of Fe^{2+} in the narsarsukite structure, but does support the results of Wagner *et al.* (1991) that at least the large majority of the iron is Fe^{3+}.

Neptunite

A study of the crystallography of neptunite, ideally $KNa_2Li(Fe,Mg,Mn)_2Ti_2Si_8O_{24}$, has been carried out by Kunz *et al.* (1991), and the geology of other occurrences reviewed by Heinrich & Quon (1963) and by Laird & Albee (1972). The composition of neptunite from Strange Lake (Table 7) shows low concentrations of Al, Sn, Zr, Ca, Zn and lanthanides. Mineral formulae, calculated from results of electron-microprobe analyses adjusted to 24 (O + F) equivalents, and with Li assumed to be 1 *apfu*, are illustrated in Table 7. Recalculations to 16 cations and to various site-filling schemes all yield broadly comparable results in terms of calculated Fe^{2+}:Fe^{3+} values. If all Fe is calculated as Fe^{2+}, an excess of cations results for most cases. To model the substitutions in neptunite, the common presence of small amounts of Nb, and the positive correlation of F and R^{3+} must be considered. The measured compositions can then be accommodated by three schemes of substitution: $R^{4+}_2(NbR^{3+})_{-1}$, $R^{4+}O(R^{3+}F)_{-1}$ and $R^{4+}R^{2+}(R^{3+})_{-2}$. An attempt to accommodate F through $R^{4+}O_2(R^{2+}F_2)_{-1}$ did not produce convincing correlations with other cations, and does not account for the positive correlation of F and Fe^{3+}. Consequently, Fe^{2+}:Fe^{3+} values were adjusted to minimize the difference between the proposed substitutions and the proportions of R^{2+} *versus* R^{4+}. The results of the calculations are illustrated in Figures 14 and 15. The Fe^{2+}:Fe^{3+} value is close to that calculated for 16 cations, or for 12 cations exclusive of Li and the sum (Na + K + Ca + Ba). The scatter (Figs. 14, 15) may result from the accumulation of analytical uncertainties on the calculated proportions of R^{3+}, or from the effects of other substitutions such as $\square OF_{-2}$ or $R^{4+}O_2(R^{2+}F_2)_{-1}$. Substantial scatter is evident in the relationship of calculated R^{3+} cations to F (Fig. 16). The good fits of the lines of Figures 14 and 15 to the analytical data support the argument that the three schemes of substitution considered here can account for the entry of "other" atoms into the structure. Since the electron microprobe cannot monitor Li, and either excess or deficiency in Li is possible with compensation by Fe^{3+} (*cf.* Hawthorne *et al.* 1993), further manipulation of the data at this stage does not seem warranted. The remaining

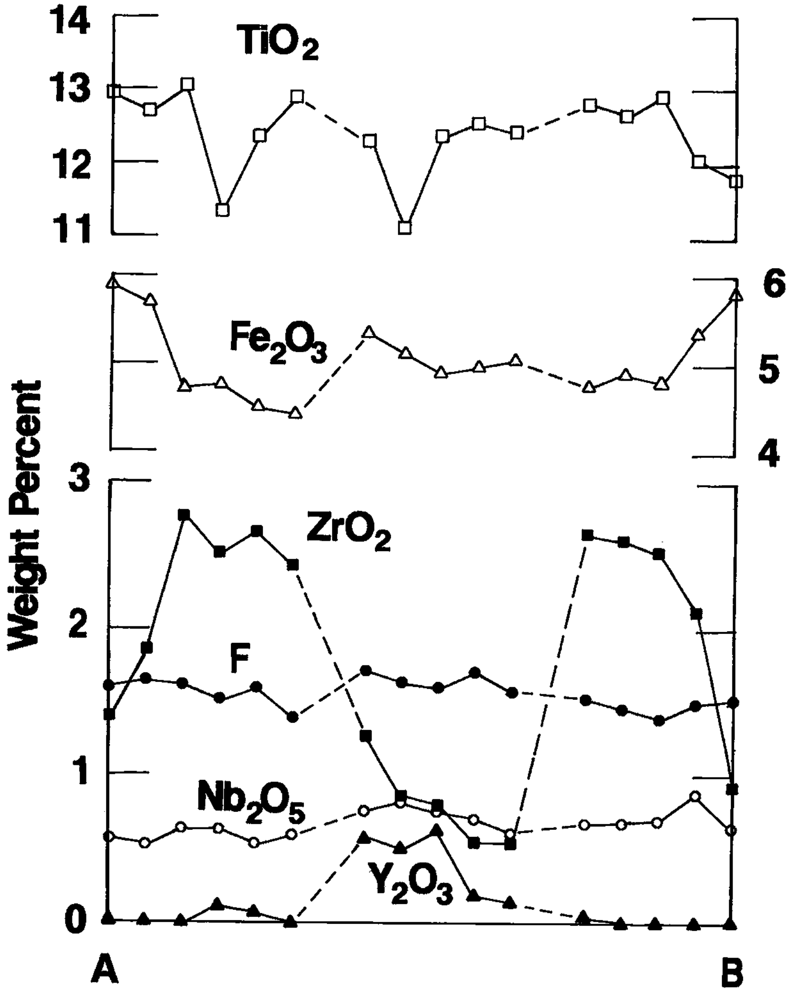

FIG. 9. Concentrations of some major elements (in weight percent of the oxides) across the narsarsukite grains along the profile of Figure 4B.

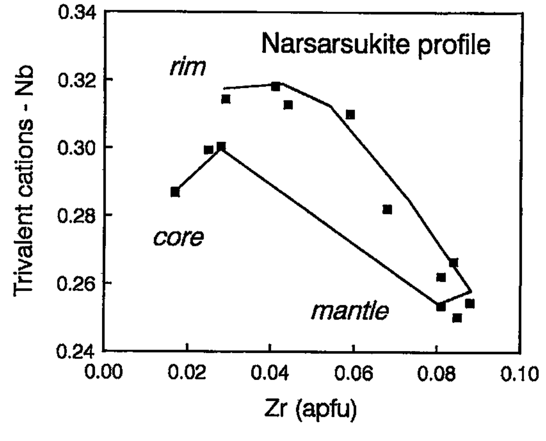

FIG. 10. Proportions of Zr atoms *versus* trivalent cations (corrected for Nb substitution) based on 11 anions for the narsarsukite compositions along the profile of Figure 5B. The distribution of R^{3+} (*apfu*) reflects the higher Fe^{3+}/Fe^{2+} or higher activity of F during the later stages of the growth of the crystal. All compositions determined from the rim and mantle of the crystal are grouped in this diagram (*i.e.*, both ends of the profile of Figure 4B).

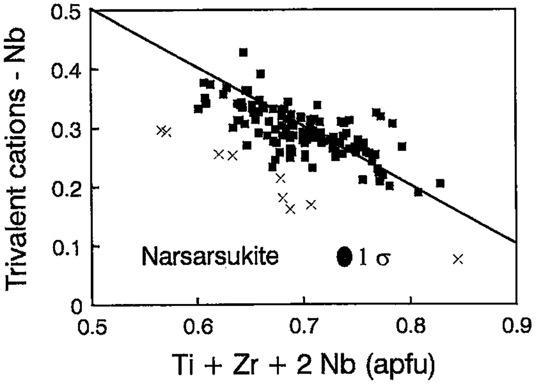

FIG. 11. Proportions of R^{3+} *versus* Ti + Zr (*apfu*) (all corrected for Nb substitution) for narsarsukite based on 11 (O + F). The line indicates a slope of –1. Symbols: ■ compositions from Strange Lake, ×: data reported by Wagner *et al.* (1991).

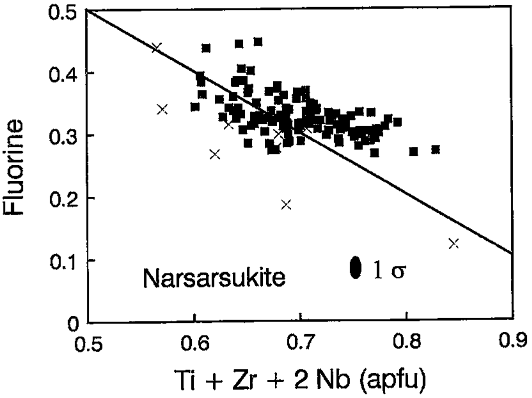

FIG. 13. Proportions of F atoms *versus* Ti + Zr (corrected for Nb substitution) for narsarsukite based on 11 (O + F). The line illustrates a slope of –1. Symbols as noted in Figure 11.

anomaly in the neptunite compositions concerns Mn, which displays a negative correlation with Fe^{2+} and a positive correlation with Fe^{3+}. The negative correlation with Fe^{2+} is the result of competition for the available sites in the neptunite structure, but there seems to be no *a priori* expectation of a positive correlation between Mn and Fe^{3+}. The data may indicate removal of Fe^{2+} from the system as other Fe^{2+}-bearing minerals crystallized; this would leave increased Fe^{3+} and Mn to enter the minerals. The neptunite from San Benito County, California (Kunz *et al.* 1991) contains nearly all Fe as Fe^{2+}, such that the proposed substitutions suggested here are new. Because possible complications regarding filling of the Si site are not addressed by this method, all of the R^{4+} cations have been considered together. A crystal-structure study of neptunite from peralkaline granites will be required before the proposed formula can be rigorously tested. The proposed incorporation of F is the same as that proposed for narsarsukite by Wagner *et al.* (1991). A formula for neptunite that accommodates F, Nb, and R^{3+} can be written $KNa_2Li(Fe^{2+},Mn,Mg)_{2-y}Nb_xFe^{3+}_{x+2y+z}Ti_{2-2x-y-z}Si_8O_{24-z}F_z$.

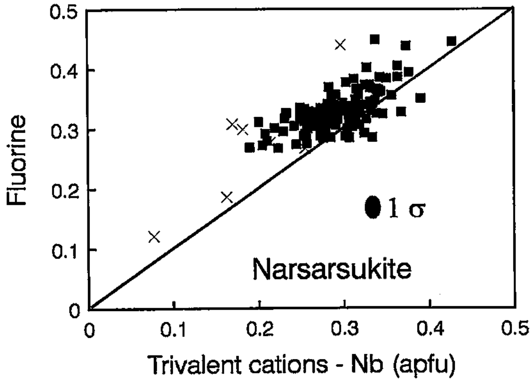

FIG. 12. Proportions of F atoms *versus* R^{3+} (corrected for Nb substitution) for narsarsukite based on 11 (O + F). There is an apparent, although relatively weak, positive corelation between the two. The line illustrates a slope of 1. The compositions of ideal narsarsukite plots at the origin. Symbols as noted Figure 11.

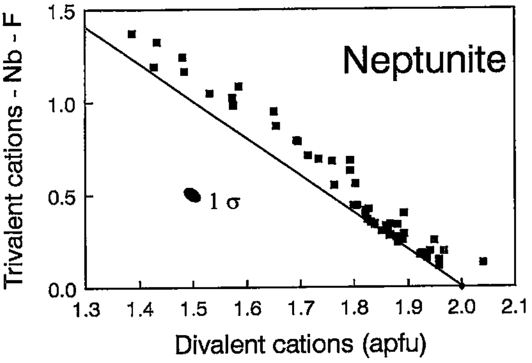

FIG. 14. Proportions of R^{3+} (corrected for Nb and F substitutions) *versus* those of divalent cations in neptunite calculated on a basis of 24 (O + F). The ideal composition of neptunite is indicated by the diamond. The line illustrates a slope of –2.

TABLE 7. NEPTUNITE COMPOSITIONS

wt.%	NF5638-9	015-A4	015-3-13	002-6	017-5	017-18	NF5879-11	NF5879-A-14
SiO_2	51.22	51.55	50.64	51.38	51.17	50.96	50.14	51.13
ZrO_2	0.01	nd	0.07	0.02	0.12	nd	0.08	0.01
TiO_2	15.38	14.75	14.71	15.99	14.60	13.51	14.00	13.58
SnO_2	0.10	0.05	0.03	0.04	0.18	0.05	0.04	0.07
Nb_2O_5	0.82	nd	0.10	0.25	0.32	0.04	nd	nd
Al_2O_3	0.05	0.19	0.40	0.13	0.09	0.07	0.10	0.10
Ce_2O_3	0.10	0.12	0.01	nd	0.16	nd	0.03	0.01
Y_2O_3	nd	nd	nd	nd	nd	nd	nd	nd
(Fe_2O_3)	2.53	3.43	4.95	2.48	3.91	7.68	10.77	7.75
FeO	13.67	15.06	13.66	13.68	13.48	12.49	9.47	12.24
MnO	0.30	0.46	0.60	0.50	0.70	0.58	1.05	1.02
MgO	0.09	0.03	0.01	0.01	0.02	nd	0.05	0.09
BaO	0.05	nd	nd	0.18	0.23	0.16	0.11	0.03
CaO	0.03	nd	nd	nd	nd	nd	0.05	0.03
ZnO	0.24	0.05	0.15	0.26	0.01	0.09	0.29	0.31
(Li_2O)	1.60	1.61	1.61	1.61	1.60	1.61	1.62	1.62
Na_2O	6.63	6.45	6.55	6.54	6.53	6.55	6.93	6.77
K_2O	5.16	5.31	4.87	5.15	4.97	4.89	4.84	4.62
F	nd	0.61	0.48	0.06	0.23	0.41	0.13	0.57
Total	97.98	99.67	98.85	98.28	98.32	99.09	99.70	99.95
-O≡F	0.00	0.26	0.20	0.03	0.10	0.17	0.05	0.24
Sum	97.98	99.42	98.64	98.26	98.23	98.92	99.64	99.71
Atoms								
Si	7.95	8.00	7.90	7.95	7.98	7.93	7.72	7.91
Zr	0.00	0	0.01	0.00	0.01	0	0.01	0.00
Ti	1.80	1.72	1.73	1.86	1.71	1.58	1.62	1.58
Sn	0.01	0.00	0.00	0.00	0.01	0.00	0.00	0.01
Nb	0.06	0	0.01	0.02	0.02	0.00	0	0
Al	0.01	0.04	0.07	0.02	0.02	0.01	0.02	0.02
Ce	0.01	0.01	0.00	0	0.01	0	0.00	0.00
Y	0	0	0	0	0	0	0	0
(Fe^{3+})	0.30	0.40	0.58	0.29	0.46	0.90	1.25	0.90
Fe^{2+}	1.78	1.96	1.78	1.77	1.76	1.63	1.22	1.58
Mn	0.04	0.06	0.08	0.07	0.09	0.08	0.14	0.13
Mg	0.02	0.01	0.00	0.00	0.01	0	0.01	0.02
Ba	0.00	0	0	0.01	0.01	0.01	0.01	0.00
Ca	0.01	0	0	0	0	0	0.01	0.01
Zn	0.03	0.01	0.02	0.03	0.00	0.01	0.03	0.04
(Li)	1.00	1.01	1.01	1.00	1.00	1.01	1.00	1.01
Na	2.00	1.94	1.98	1.96	1.97	1.98	2.07	2.03
K	1.02	1.05	0.97	1.02	0.99	0.97	0.95	0.91
F	0	0.30	0.24	0.03	0.11	0.20	0.06	0.28

Electron-microprobe analyses of neptunite calculated on a basis of 24 (O+F), 1 Li, and with Fe^{2+}, Fe^{3+} calculated as discussed in the text.

Other phases

Petrographic observations and electron-microprobe analyses have led to the recognition of two previously unknown Ti-bearing phases. One phase has been identified as inclusions in narsarsukite (Table 8, Fig. 17). This phase has a high proportion of Zr, Ca and Na, with low or negligible concentrations of Sn, Nb, Al, Fe, K and F. The low analytical totals suggest that the phase may be hydrous or contain additional light elements. Concentrations of Ti and Zr seem positively correlated.

The second, encountered in one sample (Fig. 17), has low levels of Si, Zr, Ti and Fe, high levels of Nb, Pb, and important concentrations of U and Th (Table 9). Optically, the phase is isotropic (probably metamict given the U and Th contents) and resembles pyrochlore on cursory examination. The absence of internal reflections in reflected light allows distinction from pyrochlore. Electron-probe scans (Fig. 18) indicate the presence of C in the phase (*cf.* Raudsepp 1995), but the concentration and bonding cannot be ascertained with the material presently available. Relationships of the unidentified phase to other silicocarbonate minerals are unknown. Most silicocarbonate minerals also contain H or B, or form in high-T, low-P environments (*e.g.*, spurrite, tilleyite). It is unlikely that the unidentified phase shares common features with any of these.

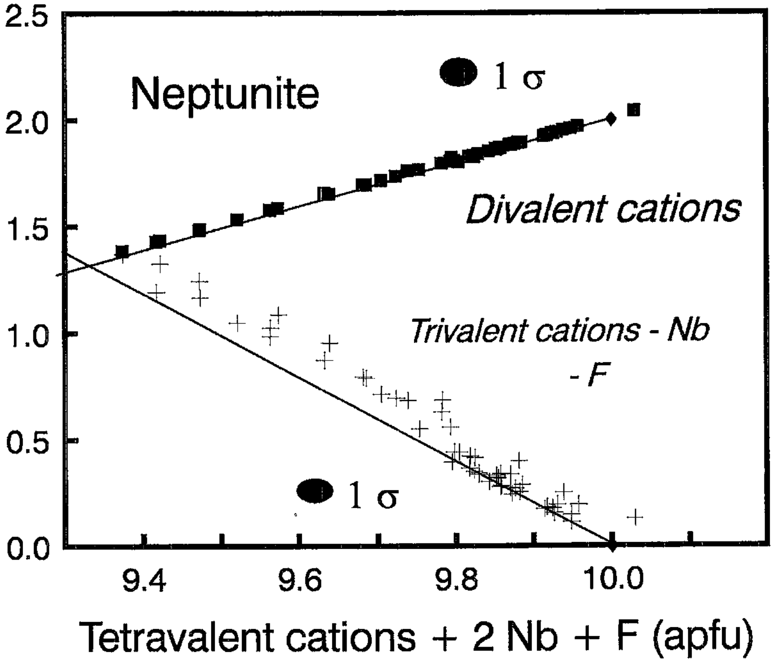

FIG. 15. A composite diagram illustrating neptunite compositions based on 24 (O + F). The abscissa represents the proportion of tetravalent cations corrected for the substitutions of Nb and F. The proportion of R^{3+} (corrected for Nb and F) and the divalent cations are plotted, as are reference lines of slopes –2 and +1. Ideal neptunite is shown by the diamonds.

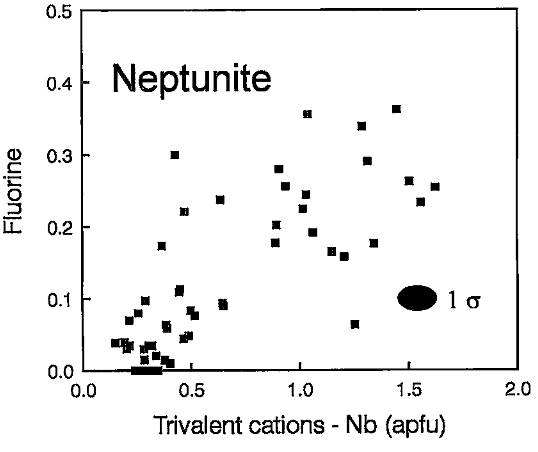

FIG. 16. The proportion of F atoms *versus* that of R^{3+} (corrected for Nb substitution) in neptunite, calculated on a basis of 24 (O + F). A weak positive corelation is evident.

TABLE 8. UNIDENTIFIED Ti–Zr–BEARING PHASE, STRANGE LAKE GRANITE

wt. %	NF5638–4	NF5638–6	NF5638–7	NF5638–18
SiO_2	50.08	53.82	48.07	59.41
ZrO_2	12.22	8.47	16.39	11.29
TiO_2	7.46	5.42	8.16	9.30
SnO_2	0.17	0.18	0.29	0.12
Nb_2O_5	1.10	0.57	1.02	0.39
Al_2O_3	0.88	0.24	0.38	0.43
Ce_2O_3	0.74	0.29	0.33	0.16
Y_2O_3	nd	1.79	nd	nd
FeO	1.88	0.70	0.80	2.56
MnO	0.07	nd	0.04	0.06
MgO	nd	nd	nd	0.01
BaO	0.23	0.16	0.20	0.08
CaO	2.90	2.61	3.96	1.37
ZnO	0.01	0.03	0.03	0.07
Na_2O	6.86	0.37	0.65	5.14
K_2O	0.28	0.76	1.39	0.05
F	1.04	0.01	0.11	0.60
Total	85.92	75.42	81.91	91.04
–O≡F	0.44	0.00	0.05	0.25
Sum	85.48	75.42	81.86	90.79
Atoms				
Si	17.59	19.70	17.33	18.63
Zr	2.09	1.51	2.88	1.73
Ti	1.97	1.49	2.21	2.19
Sn	0.03	0.03	0.05	0.02
Nb	0.18	0.09	0.17	0.06
Al	0.36	0.10	0.16	0.16
Ce	0.10	0.04	0.04	0.02
Y	0	0.35	0.02	0
Fe^{2+}	0.55	0.21	0.24	0.67
Mn	0.02	0	0.01	0.02
Mg	0	0	0	0.01
Ba	0.03	0.02	0.03	0.01
Ca	1.09	1.02	1.53	0.46
Zn	0.00	0.01	0.01	0.02
Na	4.67	0.26	0.45	3.13
K	0.13	0.36	0.64	0.02
F	1.16	0.01	0.13	0.60

Cations are calculated to a basis of 48 O atoms, all Fe as Fe^{2+}. All analyses were done in Ottawa.

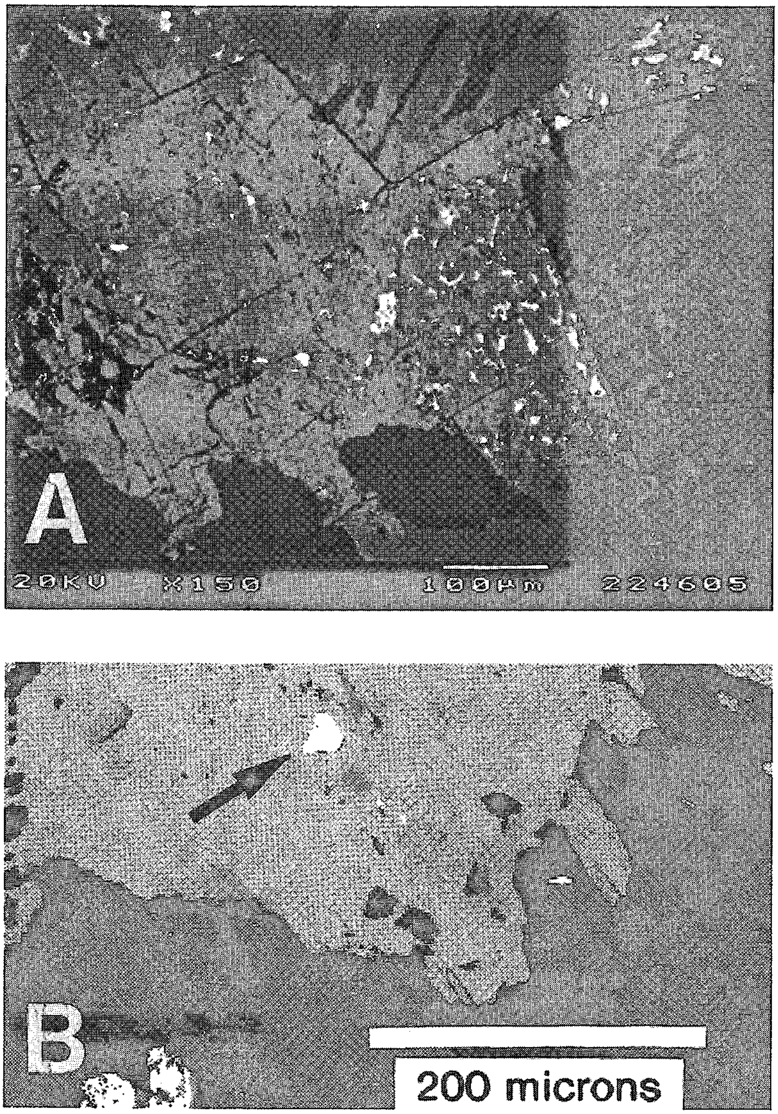

FIG. 17. A. Unidentified Ti–Zr-bearing phase. A back-scattered electron image illustrates the textures of the unidentified phase (light) in narsarsukite which, in turn, is surrounded by perthite with marginal albite (dark gray). B. Unidentified silicocarbonate (arrow) in astrophyllite surrounded by feldspar.

Mineral assemblages and reaction relationships

With the exception of bafertisite and the bafertisite-like phase, all of the Ti-bearing minerals and all of the mineral assemblages reported here coexist with quartz, fluorite, pyrochlore, and perthite or two feldspars. A Li-bearing mineral (polylithionite or neptunite) is present in all the assemblages. At Strange Lake, evidence of extensive reaction during and after initial consolidation of the granites includes: 1) amphibole partially replaced by pyroxene (and *vice versa*), 2) zircon rimmed by vlasovite or, much less commonly, by elpidite, and 3) vlasovite partially to completely replaced by catapleiite. These features occur locally even in the most primitive portions of the pluton. In the more-evolved rocks, with higher concentrations of volatiles, reactions were locally intense, with amphibole or pyroxene replaced by

TABLE 9. UNIDENTIFIED Ti–Nb–Pb–Si–C PHASE, STRANGE LAKE GRANITE

SiO_2 wt.%	19.15	ZrO_2	4.00	TiO_2	6.52
SnO_2	0.07	ThO_2	3.70	UO_2	1.51
Nb_2O_5	19.44	Al_2O_3	0.32	Ce_2O_3	2.46
Y_2O_3	nd	FeO	3.17	MnO	0.15
MgO	nd	BaO	0.24	CaO	0.74
ZnO	0.08	PbO	15.49	Na_2O	0.06
K_2O	0.13	F	0.42		
Total	77.65				
–O=F	0.18				
Sum	77.47				
(CO_2)	22.53				

Average result of two analyses (all Fe as Fe^{2+}, CO_2 by difference from 100 %).

TABLE 10. ASSEMBLAGES AND SCHEMATIC REACTIONS AMONGST THE Ti–BEARING MINERALS, STRANGE LAKE GRANITE

Stable Assemblages			Reactions				
			Ilm	→	Bft (rare)		
Ilm	+	Ang (?)	Ang	→	Ast (common)		
Ang	+	Arf	Ilm	→	Ast (common)		
Ang	+	Ast (?)	Ilm	→	Ang (?)		
Ae	+	Arf	Ang	→	Arf (common)		
Ae	+	Ast	Ang	→	Ae (common)		
Ast	+	Arf	Ang	→	Npt (local)		
Npt	+	Nrs	Npt	→	Nrs (local)		
Nrs	+	Ae	Arf	→	Npt (rare)		
Nrs	+	Arf	Ast	→	Arf (common)		
Ae	+	Hem	Ang	→	Nrs (rare)		
Nrs	+	Hem	Ast	→	Npt (rare)		
Npt	+	Arf	Ang	→	Ast	+	Arf (common)
			Ang	→	Ast	+	Ae (local)

clay minerals or prehnite. Consequently, definition of assemblages as opposed to coexistence of minerals requires a detailed examination of mineral textures. Deduced stable assemblages of precursor minerals and reactions amongst the Ti-bearing minerals are listed in Table 10. Suggested stable coexistence is based on observation of minerals in contact without apparent reaction (especially along planar boundaries), similar size-distributions, and textural relationships with other major minerals. Suggested reactions are based on rimming or veining relationships and the presence of relics of one mineral in another (with constant optical orientation of several relict mineral grains). Many early assemblages became unstable as the system evolved, and were overprinted by later assemblages. Relations of pyroxene and amphibole grains with the Ti-bearing minerals also are complicated. As the mineral textures do not provide constraints on relative volumes of reactants and products, meaningful balanced reactions among the phases cannot be recognized (*cf.* Gresens 1967).

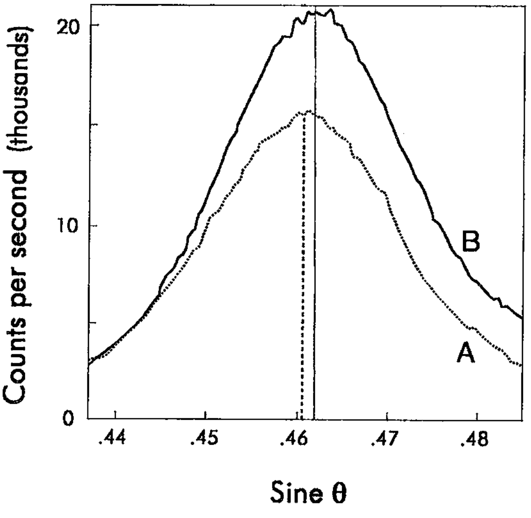

FIG. 18. Spectrometer scans (PC0 crystal) over the surrounding astrophyllite and the unidentified silicocarbonate mineral in the region of the carbon peak. The response from astrophyllite (A) is due to the carbon coating on the polished thin section, whereas the more intense peak and peak shift in B are due to the presence of carbon in the mineral.

Nicholls & Carmichael (1969) recognized the "no oxide field" in peralkaline felsic liquids, and postulated reaction relationships among ilmenite, magnetite, aenigmatite, and pyroxene with Na, Si and O from the magma. The assemblages observed at Strange Lake indicate that the early development of the rocks was at an apparently moderate oxygen fugacity, with the Fe dominantly present as Fe^{2+}, and with early-formed ilmenite present. At Strange Lake, and probably in many other alkaline complexes, the presence of other anions, in particular F, may allow substantial Fe^{3+} to be present without implying a specific oxygen fugacity. Thus, during crystallization of the Strange Lake pluton, significant Fe^{3+} was available in the melt, and the assemblage ilmenite + aenigmatite + quartz was stable at higher temperatures (above the feldspar solvus). At lower temperatures, the assemblage narsarsukite + aegirine was apparently stable (possibly with hematite) even at oxygen fugacities estimated by Salvi & Williams-Jones (1992) to be 2 to 5 log units below the quartz – fayalite – magnetite oxygen buffer based on the observation of methane-bearing fluid inclusions. The presence of the unidentified silicocarbonate mineral supports the low oxygen fugacity estimates of Salvi & Williams-Jones (1992).

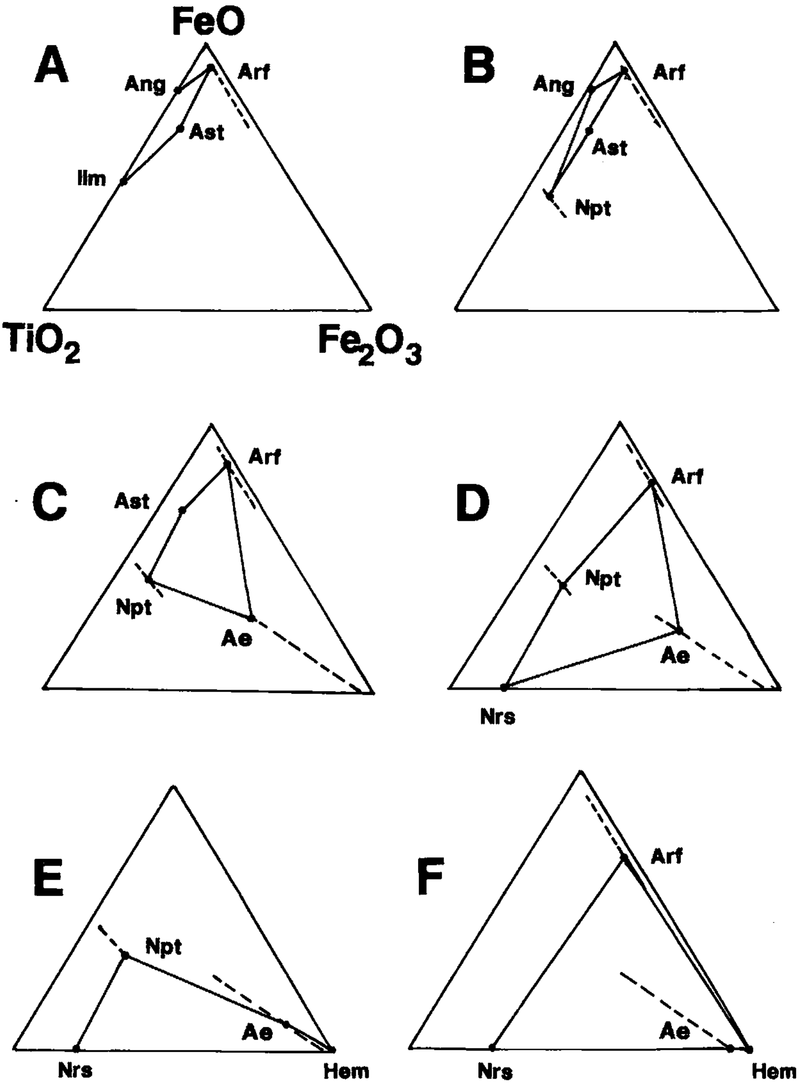

FIG. 19. Deduced mineral compatibilities illustrated in the tetrahedron Na – Fe^{2+} – Fe^{3+} – Ti. The assemblages are (A) Ilm + Arf + Ang + Ast, (B) Arf + Ang + Ast + Npt, (C) Arf + Ast + Npt + Ae, (D) Arf + Npt + Nrs + Ae, (E) Npt + Nrs + Hem + Ae, and (F) Arf + Npt + Ae + Hem. Mineral abbreviations are listed in the text.

The evolution of assemblages of Ti-bearing minerals at Strange Lake is illustrated schematically in Figure 19. Hematite, albite and end-member aegirine are colinear in this projection, as are aegirine, narsarsukite and hematite, although in nature, minor elements such as Mn increase the variance of the system. The compatibilities of Figure 19 are a suggested series of univariant assemblages. Other elements such as Ca (amphibole) or Li (amphibole and neptunite) increase the variance of the assemblages, so that four-phase associations such as illustrated are not rare. The earliest-formed Ti-bearing phase, ilmenite, was apparently joined by aenigmatite ± arfvedsonite. The ilmenite first became unstable with the magma (and possibly with aenigmatite), and bafertisite ± astrophyllite replaced it. Aenigmatite then became unstable with the magma and was replaced by astrophyllite ± arfvedsonite ± aegirine, by neptunite, or by narsarsukite. As crystallization and cooling continued, aegirine became stable relative to arfvedsonite and, in the final stages of development of the pluton, hematite formed. All of the assemblages shown in Figure 19 cannot be formed from a single bulk composition, and the mineral assemblages reflect the magmatic development of the system. Assemblages in Figure 19a to 19d were formed with perthite, whereas assemblages e and f formed with two feldspars. The assemblages of Figure 19a to e were restricted to the early granites of Figure 2, whereas the assemblage of Figure 19f formed in the middle-stage and late granites. The sequential development of minerals with higher Fe^{3+}:Fe^{2+} values was a continuous process throughout crystallization on the scale of individual samples and on the scale of the whole pluton. Although events such as loss of a fluid phase to form the fluorite breccia in the ring-fractures are recorded at Strange Lake, there is no evidence for abrupt changes in Fe^{3+}:Fe^{2+} values during cooling, as recorded in the Ti-bearing silicates. Instead, evolution of Fe^{3+}:Fe^{2+} values was a continuous process, as can be seen in the shift of the phase compatibilities away from the Ti–Fe^{2+} composition space toward the more Fe^{3+}-rich compositions in Figure 19.

DISCUSSION

Of the several substitutions discussed by Černý & Ercit (1989), $\mathrm{Nb}R^{3+}(R^{4+}_{2})_{-1}$ can account for a large proportion of Nb in astrophyllite, and probably in the other minerals considered as well. Substitutions such as $R^{4+}R^{2+}(\mathrm{NbNa})_{-1}$ generally involve Ca; this and other schemes can in some cases be eliminated because of the requirements imposed by observations of the correlations of R^{4+} and Nb.

The relationships between oxygen fugacity and the ratio of ferrous to ferric iron in magmas have been little studied with other anions added to the experiments. Mitchell & Platt (1978) and Mitchell (1990) have discussed the increasing ratio of ferric to ferrous iron in minerals of alkaline rocks with falling oxygen fugacity. Melt structure also influences the ratio of ferrous to ferric iron (Mysen *et al.* 1980, 1985, Mysen & Virgo 1989). In the Strange Lake magma, the elevated F content might have helped decouple Fe^{2+}/Fe^{3+} from oxygen fugacity, as revealed by the fluid-inclusion studies of Salvi & Williams-Jones (1992). Models requiring repeated fluctuations of oxygen fugacity during crystallization at Strange Lake (Pillet *et al.* 1993) are not supported by the progressions of mineral assemblages. Calculated constraints on oxygen fugacity using titanosilicates require correction for incorporation of ferric iron in coupled substitution with Nb (*cf.* Nicholls & Carmichael 1969, Marsh 1975).

Two models of the magmatic evolution of the Strange Lake pluton have been formulated. Pillet *et al.* (1992) considered that feldspar fractionation explains the chemical variations in the magmas, but this model does not offer adequate mass-balance for some major elements such as Fe, or for most trace elements. Boily & Williams-Jones (1994) used a combined least-squares – Rayleigh fractionation model to produce a more realistic estimate of mass balance. Both of these studies, however, would have been improved if early-crystallizing minerals such as aenigmatite were included in the calculations, rather than relatively late-crystallizing minerals such as arfvedsonite (Boily & Williams-Jones 1994). Phases not yet adequately described, such as the unidentified silicocarbonate of Table 9, may well have influenced the magmatic evolution of the pluton, particularly the trace-element budgets.

CONCLUSIONS

The entry of Nb into the Na–Ti-silicates at Strange Lake can be approximated by $\mathrm{Nb}R^{3+}(R^{4+}_{2})_{-1}$. The entry of Fe^{3+} into these minerals can be successfully modeled by substitutions such as $R^{4+}R^{2+}(R^{3+}_{2})_{-1}$. The compositional range of neptunite is extended through its incorporation of Nb, F and Fe^{3+}. Unidentified phases, including a silicocarbonate, crystallized early in the Strange Lake magma, and with other titanosilicates, may have influenced the subsequent chemical evolution of the system.

The reactions amongst the Ti-silicates considered here involved the residual magma or the immediate postmagmatic fluid. At the thin section scale of observation, the system involving the titanosilicates was open, and without an additional constraint (volume relations or robust mass-balance calculations), the actual reactions cannot be identified. The reactions took place at conditions above the feldspar solvus until the late-stage reactions involving narsarsukite took place.

The magmatic evolution at Strange Lake was toward higher Fe^{3+}: Fe^{2+} values, but no evidence of any rapid change imposed on the system is preserved in the Ti-silicates. Oxygen fugacity and Fe^{2+}/Fe^{3+} were decoupled at Strange Lake, most probably owing to the abundance of F and the effects of melt structure.

ACKNOWLEDGEMENTS

We thank M. Van Baalen and D. Lange of Harvard University and G. Pringle of the Geological Survey of Canada (GSC, Ottawa) for advice and assistance with electron-microprobe analyses. G. Ansell, GSC, provided a sample of niobophyllite from Seal Lake. Stewart Fumerton took the photograph for Figure 5A. Discussion and reviews by A.C. Roberts and W.D. Sinclair (GSC), P. Černý, R. Mitchell, R.F. Martin and an anonymous reviewer improved the presentation of ideas. W.E.T.Jr. acknowledges support by the Natural Sciences and Engineering Research Council of Canada.

REFERENCES

ABDEL-RAHMAN, A. (1992): Mineral chemistry and paragenesis of astrophyllite from Egypt. *Mineral. Mag.* **56**, 17-26.

BIRKETT, T.C. & MILLER, R.R. (1991): Comment on "The role of hydrothermal processes in the granite-hosted Zr, Y, REE deposit at Strange Lake, Quebec/Labrador: evidence from fluid inclusions" by S. Salvi and A.E. Williams-Jones. *Geochim. Cosmochim. Acta* **55**, 3443-3445.

________, ________, ROBERTS, A.C. & MARIANO, A.N. (1992): Zirconium-bearing minerals of the Strange Lake Intrusive Complex, Quebec–Labrador. *Can. Mineral.* **30**, 191-205.

BOILY, M. & WILLIAMS-JONES, A.E. (1994): The role of magmatic and hydrothermal processes in the chemical evolution of the Strange Lake plutonic complex, Québec–Labrador. *Contrib. Mineral. Petrol.* **118**, 33-47.

BURT, D.M. (1988): Vector representation of phyllosilicate compositions. *In* Micas (S.W. Bailey, ed.). *Rev. Mineral.* **19**, 561-599.

________ (1989): Vector representation of tourmaline compositions. *Am. Mineral.* **74**, 826-839.

________ (1994): Vector representation of some mineral compositions in the aenigmatite group, with special reference to høgtuvaite. *Can. Mineral.* **32**, 449-457.

ČERNÝ, P. & ERCIT, T.S. (1989): Mineralogy of niobium and tantalum: crystal chemical relationships, paragenetic aspects and their economic implications. *In* Lanthanides, tantalum and niobium (P. Möller, P. Černý & F. Saupé, eds.). SGA Spec. Publ. **7**, 27-79. Springer Verlag, Berlin, Germany.

COSCA, M.A., ROUSE, R.C. & ESSENE, E.J. (1988): Dorrite $[Ca_2(Mg_2Fe^{3+}_4)(Al_4Si_2)O_{20}]$, a new member of the aenigmatite group from a pyrometamorphic melt-rock. *Am. Mineral.* **73**, 1440-1448.

CURRIE, K.L. (1985): An unusual peralkaline granite near Lac Brisson, Quebec–Labrador. *Geol. Surv. Can., Pap.* **85-1A**, 73-80.

DUGGAN, M.B. (1990): Wilkinsonite, $Na_2Fe^{2+}_4Fe^{3+}_2Si_6O_{20}$, a new member of the aenigmatite group from the Warrumbungle Volcano, New South Wales, Australia. *Am. Mineral.* **75**, 694-701.

GREEN, T.H. & PEARSON, N.J. (1987): An experimental study of Nb and Ta partitioning between Ti-rich minerals and silicate liquids as high pressure and temperature. *Geochim. Cosmochim. Acta* **51**, 55-62.

GRESENS, R.L. (1967): Composition – volume relationships of metasomatism. *Chem. Geol.* **2**, 47-65.

HAWTHORNE, F.C., UNGARETTI, L., OBERTI, R., BOTTAZZI, P. & CZAMANSKE, G.K. (1993): Li: an important component of igneous alkali amphiboles. *Am. Mineral.* **78**, 733-745.

HEINRICH, E.W. & QUON, S.H. (1963): Neptunite from Seal Lake, Labrador. *Can. Mineral.* **7**, 650-654.

JAMBOR, J.L., ROBERTS, A.C. & GRICE, J.D. (1987): Armstrongite from the Strange Lake alkalic complex on the Quebec–Labrador boundary, Canada. *Powder Diffraction* **2**, 2-4.

KRETZ, R. (1983): Symbols for rock-forming minerals. *Am. Mineral.* **68**, 277-279.

KUNZ, M., ARMBRUSTER, T., LAGER, G.A., SCHULTZ, A.J., GOYETTE, R.J., LOTTERMOSER, W. & AMTHAUER, G. (1991): Fe, Ti ordering and octahedral distorsions in acentric neptunite: temperature dependent X-ray and neutron structure refinements and Mössbauer spectroscopy. *Phys. Chem. Minerals* **18**, 199-213.

LAIRD, J. & ALBEE, A.A. (1972): Chemical composition and physical, optical, and structural properties of benitoite, neptunite, and joaquinite. *Am. Mineral.* **57**, 85-102.

LARSEN, A.O., RAADE, G. & SAEBO, P.C. (1992): Lorenzenite from the Bratthagen nepheline syenite pegmatites, Lågendalen, Oslo region, Norway. *Norsk Geol. Tidsskr.* **72**, 381-384.

LAYNE, G.D., RUCKLIDGE, J.C. & BROOKS, C.K. (1982): Astrophyllite from Kangerdlugssuaq, East Greenland. *Mineral. Mag.* **45**, 149-156.

MACDONALD, R. & SAUNDERS, M.J. (1973): Chemical variations in minerals of the astrophyllite group. *Mineral. Mag.* **39**, 97-111.

MARSH, J.S. (1975): Aenigmatite stability in silica-undersaturated rocks. *Contrib. Mineral. Petrol.* **50**, 135-144.

MARTIN, D. (1975): *Studies of Astrophyllite from Mont St. Hilaire, Quebec.* B.Sc. thesis, Carleton University, Ottawa, Ontario.

MAUGER, R.L. (1983): Bafertisite and an unidentified BaCaMnFeTi silicate from Fountain Quarry, Pitt County, North Carolina. *Southeastern Geology* **24**, 13-20.

MILLER, R.R. (1985): Geology of the Strange Lake alkalic complex and the associated Zr–Y–Nb–Be–REE mineralization. *In* Granite-Related Mineral Deposits; Geology, Petrogenesis and Tectonic Setting (R.P. Taylor & D.F. Strong, eds.). *Can. Inst. Mining Metall., Extended Abstr.*, 193-196.

________ (1986): Geology of the Strange Lake alkalic complex and the associated Zr–Y–Nb–Be–REE mineralization. *Newfoundland Dep. Mines, Mineral Development Div., Current Res., Rep.* **86-1**, 11-19.

________ (1988): Yttrium (Y) and other rare metals (Be, Nb, Ta, Zr) in Labrador. *Newfoundland Dep. Mines, Mineral Development Div., Current Res., Rep.* **88-1**, 229-245.

________ (1990): The Strange Lake pegmatite-aplite hosted rare-metal deposit, Labrador. *Newfoundland Dep. Mines and Energy, Geol. Surv. Branch, Rep.* **90-1**, 171-182.

Mitchell, R.H. (1990): A review of the compositional variation of amphiboles in alkaline plutonic complexes. *Lithos* **26**, 135-156,

________ & Platt, G.R. (1978): Mafic mineralogy of ferroaugite syenite from the Coldwell alkaline complex, Ontario, Canada. *J. Petrol.* **19**, 627-651.

Mysen, B.O., Seifert, F. & Virgo, D. (1980): Structure and redox equilibria of iron-bearing silicate melts. *Am. Mineral.* **65**, 867-884.

________ & Virgo, D. (1989): Redox equilibria, structure, and properties of Fe-bearing aluminosilicate melts: relationships among temperature, composition and oxygen fugacity in the system $Na_2O - Al_2O_3 - SiO_2 - Fe - O$. *Am. Mineral.* **74**, 58-76.

________, ________, Neumann, E.-R. & Seifert, F.A. (1985): Redox equilibria and the structural states of ferric and ferrous iron in melts in the system $CaO - MgO - Al_2O_3 - SiO_2 - Fe - O$: relationships between redox equilibria, melt structure and liquidus phase equilibria. *Am. Mineral.* **70**, 317-331.

Nassif, G.J. (1993): *The Strange Lake Peralkaline Complex, Québec–Labrador: the Hypersolvus – Subsolvus Granite Transition and Feldspar Mineralogy.* M.Sc. thesis, McGill Univ., Montreal, Quebec.

________ & Martin, R.F. (1991): The hypersolvus granite – subsolvus granite transition at Strange Lake, Quebec–Labrador. *Geol. Assoc. Can. – Mineral. Assoc. Can., Abstr. Program* **16**, A89.

________ & ________ (1992): Feldspar mineralogy of the Strange Lake peralkaline complex, Quebec–Labrador. *Geol. Assoc. Can. – Mineral. Assoc. Can., Abstr. Program* **17**, A83.

Nicholls, J. & Carmichael, I.S.E. (1969): Peralkaline acid liquids: a petrological study. *Contrib. Mineral. Petrol.* **20**, 268-294.

Nickel, E.H., Rowland, J.F. & Charette, D.J. (1964): Niobophyllite – the niobium analogue of astrophyllite; a new mineral from Seal Lake, Labrador. *Can. Mineral.* **8**, 40-52.

Pillet, D. (1989): *Le granite peralcalin du lac Brisson, Labrador Central (Province du Québec, Canada). Pétrologie, géochronologie, et relations avec les minéralisations internes à Zr, Y, Nb.* Thèse de doctorat, Université Claude-Bernard – Lyon I, Lyon, France.

________, Chenevoy, M. & Bélanger, M. (1992): Pétrologie du granite peralcalin du lac Brisson, Labrador central, Nouveau-Québec. I. Mode de mise en place et évolution chimique. *Can. J. Earth Sci.* **29**, 353-372.

________, ________ & ________ (1993): Pétrologie du granite peralcalin du lac Brisson, Labrador central, Nouveau-Québec. II. Minéralogie et modalités de cristallisation. *Can. J. Earth Sci.* **30**, 2423-2435.

Pouchou, J.L. & Pichoir, F. (1985): "PAP" $\varphi(\rho z)$ procedure for improved quantitative microanalysis. *Microbeam Anal.* **20**, 104-106.

Raudsepp, M. (1995): Recent advances in the electron-probe microanalysis of minerals for the light elements. *Can. Mineral.* **33**, 203-218.

Roelofsen-Ahl, J.N. & Peterson, R.C. (1989): Gittinsite, a modification of the thortveiiite structure. *Can. Mineral.* **27**, 703-708.

Salvi, S. & Williams-Jones, A.E. (1990): The role of hydrothermal processes in the granite-hosted Zr, Y, REE deposit at Strange Lake, Quebec/Labrador: evidence from fluid inclusions. *Geochim. Cosmochim. Acta* **54**, 2403-2418.

________ & ________ (1991): Reply to Comment by T.C. Birkett and R.R. Miller on "The role of hydrothermal processes in the granite-hosted Zr, Y, REE deposit at Strange Lake, Quebec/Labrador: evidence from fluid inclusions". *Geochim. Cosmochim. Acta* **55**, 3447-3449.

________ & ________ (1992): Reduced orthomagmatic C–O–H–N–NaCl fluids in the Strange Lake rare-metal granitic complex, Quebec/Labrador, Canada. *Eur. J. Mineral.* **4**, 1155-1174.

Vrána, S., Rieder, M. & Gunter, M.E. (1992): Hejtmanite, a manganese-dominant analogue of bafertisite, a new mineral. *Eur. J. Mineral.* **4**, 35-43.

Wagner, C., Parodi, G.C., Semet, M., Robert, J.-L., Berrahma, M. & Velde, D. (1991): Crystal chemistry of narsarsukite. *Eur. J. Mineral.* **3**, 575-585.

Zajac, I.S., Miller, R.R., Birkett, T.C. & Nantel, S. (1984a): The Strange Lake deposit, Quebec-Labrador. *Can. Inst. Mining Metall., Bull.* **77**(863), 60 (abstr.).

________, ________, ________ & ________ (1984b): Le gîte de Zr, Y, Nb et Be du complex alcalin de Strange Lake, Québec–Labrador. *Québec Ministère de l'Energie et des Ressources* **DV 84-18**, 127-142.

Received August 6, 1995, revised manuscript accepted April 5, 1996.